# Cyclometalated Iridium(III) Bipyridyl–Phenylenediamine Complexes with Multicolor Phosphorescence: Synthesis, Electrochemistry, Photophysics, and Intracellular Nitric Oxide Sensing

Wendell Ho-Tin Law, Kam-Keung Leung, Lawrence Cho-Cheung Lee, Che-Shan Poon, Hua-Wei Liu, and Kenneth Kam-Wing Lo*[a]

We present a new class of phosphorescent cyclometalated iridium(III) bipyridyl–phenylenediamine complexes [Ir(N^C)$_2$(bpy-DA)](PF$_6$) (bpy-DA = 4-(N-(2-amino-5-methoxyphenyl)aminomethyl)-4′-methyl-2,2′-bipyridine; HN^C = 2-(2,4-difluorophenyl)pyridine (Hdfppy) (1a), 2-phenylpyridine (Hppy) (2a), 2-phenylquinoline (Hpq) (3a), 2-phenylcinchoninic acid methyl ester (Hpqe) (4a)) and their triazole counterparts [Ir(N^C)$_2$(bpy-T)](PF$_6$) (bpy-T = 4-((6-methoxybenzotriazol-1-yl)methyl)-4′-methyl-2,2′-bipyridine; HN^C = Hdfppy (1b), Hppy (2b), Hpq (3b), Hpqe (4b)). Upon photoexcitation, the diamine complexes exhibited fairly weak green to red phosphorescence under ambient conditions whereas the triazole derivatives emitted strongly. The photophysical properties of complexes 2a and 2b have been studied in more detail. Upon protonation, the diamine complex 2a displayed increased emission intensity, but the emission properties of its triazole counterpart complex 2b were independent on the pH value of the solution. Also, complex 2a was found to be readily converted into complex 2b upon reaction with NO under aerated conditions, resulting in substantial emission enhancement of the solution. The reaction was highly specific toward NO over other reactive oxygen and nitrogen species (RONS) as revealed by spectroscopic analyses. The lipophilicity and cellular uptake efficiency of the diamine complexes have been examined and correlated to their molecular structures. Also, cell-based assays showed that these complexes were noncytotoxic toward human cervix epithelioid carcinoma (HeLa) cells (at 10 μm, 4 h, percentage survival ≈80–95%). Additionally, the diamine complexes have been used to visualize intracellular NO generated both exogenously in HeLa cells and endogenously in RAW 264.7 murine macrophages by laser-scanning confocal microscopy.

## Introduction

Nitric oxide (NO) is a reactive, ubiquitous, and paramagnetic free radical that has attracted much attention since its discovery as an endothelium-derived relaxing factor (EDRF).[1] It is produced endogenously in mammalian cells by three nitric oxide synthase (NOS): neuronal NOS (nNOS), endothelial NOS (eNOS), and inducible NOS (iNOS), all of which catalyze the conversion of L-arginine to NO and L-citrulline.[2] Other reports have revealed that NO plays a key role in the signaling processes of immune, cardiovascular, and nervous systems.[1e, 2b, 3] Unregulated NO production may be associated with various diseases such as cancer, septic shock, Alzheimer's, Parkinson's, and Huntington's disease.[4] For these reasons, the development of sensors to detect intracellular NO is of paramount importance. Up to date, various techniques including colorimetry,[5] electrochemistry,[6] fluorometry,[2c, 7] electron-paramagnetic resonance,[2c, 8] and chemiluminescence[9] have been reported. Among them, fluorometric analysis that utilizes molecular probes is regarded as the most ideal method for in vitro and in vivo NO detection.[2c, 7e]

To date, fluorometric detection of NO has basically relied on two strategies. The first one is the exploitation of a paramagnetic metal ion such as copper(II) as a quencher for a fluorescent ligand. After the metal ion is reduced by NO and displaced from the ligand, the fluorescence is restored.[7a,c,h,i] The second strategy involves the photoinduced electron transfer (PeT) quenching of a fluorophore by an electron-rich o-phenylenediamine moiety, which also acts as a NO-sensing unit.[2c, 7e,k,l] Emission enhancement is observed when the o-phenylenediamine moiety is converted to an electron-deficient benzotriazole derivative by NO under aerobic conditions (Scheme 1). Based on this strategy, the o-phenylendiamine moiety has been conjugated to a number of organic fluorophores to afford NO sensors; examples include diaminofluorescein (DAF),[10] diaminorhodamine (DAR),[11] diamino-BODIPY (DAMBO),[12] dichlorodiaminocalcein (DCl-DA Cal),[13] and the near-IR and two-photon absorbing dyes diaminocyanine (DAC),[14] ANO1,[7k] and Lyso-NINO.[7l] Despite these reports, phosphorescent transition metal complexes that can be ap-

[a] W. H.-T. Law, K.-K. Leung, L. C.-C. Lee, C.-S. Poon, Dr. H.-W. Liu, Prof. K. K.-W. Lo
Department of Biology and Chemistry
City University of Hong Kong
Tat Chee Avenue, Kowloon, Hong Kong (P.R. China)
E-mail: bhkenlo@cityu.edu.hk
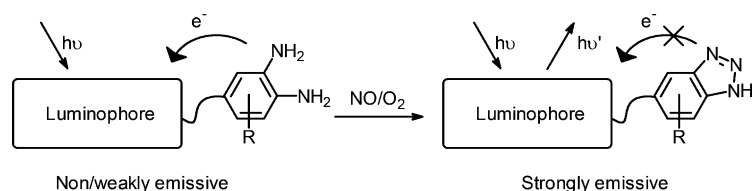
**Scheme 1.** Schematic representation of NO sensing by luminescent *o*-phenylenediamine derivatives.

plied to detect NO in living species have been scarce.[15] In consideration of the interesting photophysical behavior such as intense and long-lived emission, high photostability, and high environment sensitivity of cyclometalated iridium(III) polypyridine complexes, we anticipate that modification of these complexes with an *o*-phenylenediamine unit will generate a new class of phosphorescent molecular probes for NO.

Herein, we present the synthesis and characterization of a class of phosphorescent cyclometalated iridium(III) bipyridyl–



**Figure 1.** Structures of complexes **1a**–**4a** and **1b**–**4b**.

phenylenediamine complexes [Ir(N^C)$_2$(bpy-DA)](PF$_6$) (bpy-DA = 4-(*N*-(2-amino-5-methoxyphenyl)amino-methyl)-4′-methyl-2,2′-bipyridine; HN^C = 2-(2,4-difluorophenyl)pyridine (Hdfppy) (**1a**), 2-phenylpyridine (Hppy) (**2a**), 2-phenylquinoline (Hpq) (**3a**), 2-phenylcinchoninic acid methyl ester (Hpqe) (**4a**)) (Figure 1). Their triazole counterparts [Ir(N^C)$_2$(bpy-T)](PF$_6$) (bpy-T = 4-((6-methoxybenzotriazol-1-yl)methyl)-4′-methyl-2,2′-bipyridine; HN^C = Hdfppy (**1b**), Hppy (**2b**), Hpq (**3b**), Hpqe (**4b**)) have also been prepared. The electrochemical and photophysical properties of the complexes have been studied. The emission responses of the ppy complexes **2a** and **2b** at different pH values have been examined. The NO-sensing properties and selectivity of complex **2a** over other reactive oxygen and nitrogen species (RONS) have also been investigated. The lipophilicity of the diamine complexes has been determined using the flask-shaking method. Also, the cellular uptake efficiency of these complexes has been examined by inductively coupled plasma mass spectroscopy (ICP-MS) using human cervix epithelioid carcinoma (HeLa) as a model cell line. Additionally, the cytotoxic activity of the diamine complexes toward HeLa cells has been evaluated by the 3-(4,5-dimethyl-2-thiazolyl)-2,5-diphenyltetrazolium bromide (MTT) assay. Furthermore, live-cell images of NO generated both exogenously in HeLa cells and endogenously in RAW 264.7 murine marcophages have been investigated by laser-scanning confocal microscopy.

## Results and Discussion

### Synthesis

The bipyridine derivative 4-(*N*-(2-(*N*-*tert*-butoxycarbonylamino)-5-methoxyphenyl)aminomethyl)-4′-methyl-2,2′-bipyridine (bpy-DA-Boc) was prepared by reductive amination of 4-formyl-4′-methyl-2,2′-bipyridine (bpy-CHO) with 2-(*N*-*tert*-butoxycarbonylamino)-5-methoxyaniline. The methoxy group was added to enhance the electron density of the phenyl ring and hence the reactivity of the diamines toward NO.[7e, 12a, 15a,b] Reaction of [Ir$_2$-(N^C)$_4$Cl$_2$] (HN^C = Hdfppy, Hppy, Hpq, and Hpqe) with bpy-DA-Boc in a mixture of CH$_2$Cl$_2$/methanol, followed by anion exchange with KPF$_6$, purification by column chromatography, and recrystallization from CH$_2$Cl$_2$/diethyl ether gave the complexes [Ir(N^C)$_2$(bpy-DA-Boc)](PF$_6$) as brown crystals. Deprotection of the diamine moiety using trifluoroacetic acid (TFA) and subsequent recrystallization from CH$_2$Cl$_2$/diethyl ether afforded complexes **1a**–**4a** as brown crystals. The triazole derivatives **1b**–**4b** were synthesized by reaction of the respective diamine complexes with NO gas under aerated conditions. They were purified by column chromatography and recrystallized from CH$_2$Cl$_2$/diethyl ether and isolated as yellow to red crystals. Interestingly, the chemical shifts of the *CH*$_2$N moiety on the bipyridine ligand of the triazole complexes ($\delta \approx 5.96$-6.14 ppm) occurred at lower field than those of the respective diamine complexes ($\delta \approx 4.46$-4.63 ppm) as a consequence of the electron-withdrawing properties of the triazole moiety.
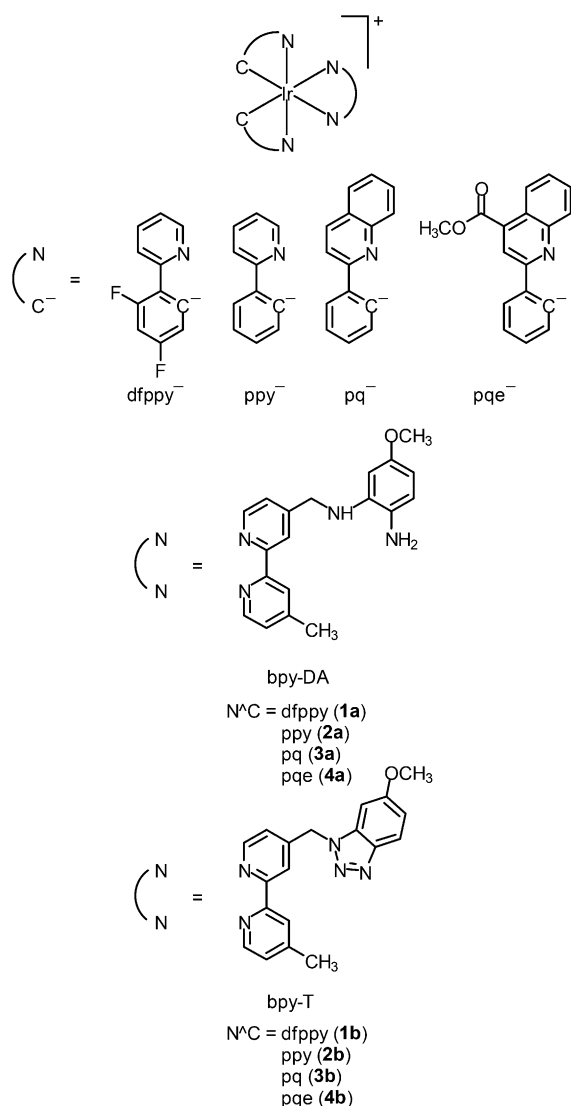
## Electrochemical properties

The electrochemical properties of all complexes were investigated by cyclic voltammetry, and the electrochemical data are summarized in Table 1. Complexes **1a**–**4a** and **1b**–**4b** exhibit-

| Table 1. Electrochemical data of iridium(III) complexes at 298 K.[a] | | |
|---|---|---|
| Complex | Oxidation ($E_{1/2}$ or $E_a$) [V] | Reduction ($E_{1/2}$ or $E_c$) [V] |
| **1a** | +0.43,[b] +1.17,[b] +1.57[c] | −1.40, −1.96,[b] −2.09,[c] −2.44[b] |
| **1b** | +1.56[c] | −1.32, −1.94,[b] −2.08, −2.36,[c] −2.61[b] |
| **2a** | +0.41,[c] +1.10,[c] +1.25[c] | −1.45, −2.00,[c] −2.21, −2.46 |
| **2b** | +1.24[c] | −1.36, −1.97,[c] −2.18, −2.48 |
| **3a** | +0.43,[b] +1.13,[b] +1.27[c] | −1.47, −1.75, −1.97,[c] −2.42[c] |
| **3b** | +1.27[c] | −1.38, −1.75, −1.98,[c] −2.32[c] |
| **4a** | +0.42,[b] +1.18,[b] +1.35[c] | −1.11, −1.27, −1.76,[c] −2.19,[b] −2.60[b] |
| **4b** | +1.35[c] | −1.10, −1.26,[c] −1.67,[c] −2.20,[b] −2.58[b] |
| [a] In CH₃CN (0.1 M TBAP), glassy carbon electrode, sweep rate = 100 mVs⁻¹, all potentials are versus SCE. [b] Irreversible waves. [c] Quasi-reversible couples. | | |

ed a quasi-reversible oxidation couple at +1.24 to +1.57 V versus SCE, which has been assigned to a metal-centered iridium(IV)/(III) oxidation process.[16] These potentials follow the orders: **2a** < **3a** < **4a** < **1a** and **2b** < **3b** < **4b** < **1b**, which are in agreement with the increasing electron-withdrawing effect of the cyclometalating ligands. The diamine complexes **1a**–**4a** displayed two additional quasi-reversible couples or irreversible waves at ≈ +0.41 to +1.18 V, which were absent in the triazole complexes **1b**–**4b**. These features have been attributed to the oxidation of the diamine units. The first reduction couples of complexes **1a**–**3a** and **1b**–**3b** were reversible in nature and occurred at ≈ −1.32 to −1.47 V, which should be associated with the reduction of diimine ligands.[16,17] This is in accordance with the fact that the electron-withdrawing properties of the triazole moiety rendered the reduction of the triazole complexes **1b**–**3b** to occur at less negative potentials (−1.32 to −1.38 V) compared with the corresponding diamine complexes (−1.40 to −1.47 V). It is noteworthy that the first reduction potentials of the pqe complexes **4a** and **4b** were very similar (−1.11 and −1.10 V) and less negative than those of other complexes. Thus, it is conceivable that the first reversible reduction couples of these two complexes are associated with the cyclometalating ligand pqe.

## Photophysical properties

The electronic absorption spectral data of the iridium(III) complexes in CH₂Cl₂ and CH₃CN at 298 K are listed in Table 2. The electronic absorption spectra of the diamine complexes **1a**–**4a** in CH₂Cl₂ at 298 K are shown in Figure 2. All of the iridium(III) complexes showed intense spin-allowed intraligand (¹IL) (π→ π*) (N^C and N^N)) absorption features in the UV region (≈254–376 nm, $\varepsilon$ in the order of $10^4$ dm³mol⁻¹cm⁻¹) and weaker spin-allowed metal-to-ligand charge-transfer (¹MLCT) (dπ(Ir)→π*(N^N and N^C)) absorption shoulders or bands in the visible region (≳ 366 nm).[16–18] The weaker absorption tail-

ing beyond ≈421 nm has been assigned to spin-forbidden ³MLCT (dπ(Ir)→π*(N^N and N^C)) transitions.[16–18]

Photoexcitation of the complexes resulted in green to red emission in fluid solutions under ambient conditions and in low-temperature alcohol glass. The photophysical data are listed in Table 3 and the emission spectra of the diamine complexes **1a**–**4a** in CH₂Cl₂ at 298 K are shown in Figure 3. The dfppy (**1a** and **1b**) and ppy (**2a** and **2b**) complexes showed a structureless emission band with positive solvatochromism in fluid solutions at 298 K. Also, there were significant blueshifts of the emission maxima of these complexes upon cooling the samples to 77 K. With reference to the previous photophysical studies on related phosphorescent cyclometalated iridium(III) complexes,[16a,c,17a,18,19] the emission of these complexes has been ascribed to a ³MLCT (dπ(Ir)→π*(N^N)) excited state. Similar to the dfppy and ppy analogues, the emission maxima of the pqe complexes **4a** and **4b** were also structureless, and redshifted upon increasing the polarity of the solvent. We have tentatively assigned the emission to an excited state of ³MLCT (dπ(Ir)→π*(pqe)) character.[16d] Unexpectedly, complex **4b** displayed dual emission in degassed buffer solution with high-energy (HE) and low-energy (LE) features at ≈529 nm and 653 nm, respectively

| Table 2. Electronic absorption spectral data of iridium(III) complexes at 298 K. | | |
|---|---|---|
| Complex | Solvent | $\lambda_{abs}$ [nm] ($\varepsilon$ [dm³mol⁻¹cm⁻¹]) |
| **1a** | CH₂Cl₂ | 267 sh (67,615), 309 sh (39,710), 366 sh (10,960), 501 sh (1,530) |
| | CH₃CN | 267 sh (54,745), 297 (35,950), 314 sh (27,345), 366 sh (8,110), 501 sh (1,205) |
| **1b** | CH₂Cl₂ | 268 sh (56,610), 296 (37,810), 314 sh (25,390), 370 sh (7,175), 426 sh (1,290), 451 sh (770) |
| | CH₃CN | 266 sh (61,205), 289 (39,675), 295 (40,005), 313 sh (26,165), 367 sh (7,045), 421 sh (1,400), 449 sh (645) |
| **2a** | CH₂Cl₂ | 258 (65,120), 278 sh (53,315), 308 sh (31,820), 340 sh (12,630), 381 (8,545), 415 sh (5,100), 469 (1610) |
| | CH₃CN | 254 (61,950), 278 sh (44,030), 308 sh (29,635), 340 sh (11,450), 381 (6,960), 415 sh (4,250), 468 (1,280) |
| **2b** | CH₂Cl₂ | 263 (63,740), 295 (42,455), 311 sh (26,535), 338 sh (11,800), 382 (8,350), 410 sh (4,915), 470 (1,030) |
| | CH₃CN | 261 (64,180), 295 (40,205), 311 sh (25,660), 338 sh (11,655), 380 (7,595), 410 sh (4,500), 469 (950) |
| **3a** | CH₂Cl₂ | 263 sh (51,595), 281 (52,725), 310 sh (25,735), 337 (23,910), 353 sh (20,555), 441 (5,730), 514 sh (1,000) |
| | CH₃CN | 260 sh (53,700), 270 (53,680), 302 sh (28,995), 335 (23,925), 351 sh (20,005), 438 (5,580), 510 sh (1,060) |
| **3b** | CH₂Cl₂ | 264 (52,955), 281 (57,780), 294 (37,010), 340 (23,135), 363 sh (13,675), 439 (5,405), 510 sh (720) |
| | CH₃CN | 262 sh (57,040), 276 (59,555), 293 (37,365), 337 (23,685), 360 sh (14,370), 435 (5,520), 506 sh (768) |
| **4a** | CH₂Cl₂ | 267 (55,110), 293 (53,940), 308 sh (31,455), 345 sh (26,340), 376 (23,715), 471 (5,705) |
| | CH₃CN | 265 (55,140), 290 (51,715), 307 sh (31,645), 343 sh (26,220), 371 (23,350), 470 (5,695) |
| **4b** | CH₂Cl₂ | 266 (46,360), 292 (45,980), 311 sh (21,245), 347 sh (21,645), 374 (20,925), 477 sh (4,210) |
| | CH₃CN | 266 (56,465), 288 (54,290), 311 sh (25,230), 342 sh (25,545), 373 (23,195), 477 sh (4,720) |
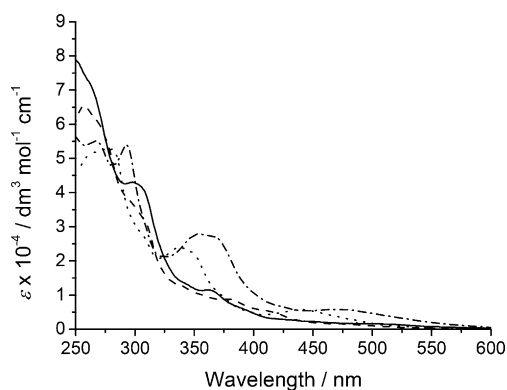
**Figure 2.** Electronic absorption spectra of complexes **1a** (——), **2a** (– – –), **3a** (••••), and **4a** (–•–•) in CH$_2$Cl$_2$ at 298 K.
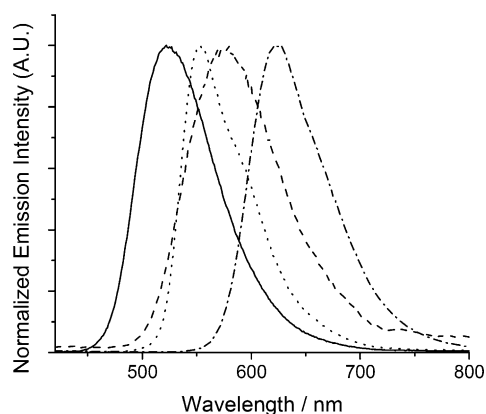


**Figure 3.** Emission spectra of complexes **1a** (——), **2a** (– – –), **3a** (••••), and **4a** (–•–•) in CH$_2$Cl$_2$ at 298 K.

(Table 3). On the basis of the extended π conjugation of pqe and the relatively longer emission lifetimes (0.83 μs), the HE feature has been assigned to a $^3$IL (π→π*) (pqe) emissive state. The LE feature with a shorter emission lifetime (≈0.48 μs) in aqueous buffer than in less polar CH$_3$CN (≈0.71 μs) should originate from a $^3$CT state, which is $^3$MLCT

and ligand-to-ligand charge-transfer ($^3$LLCT) (π(pqe)→π*(bpy-T)) in nature.[20] In contrast, the pq complexes (**3a** and **3b**) showed vibronically structured emission features at ≈552–556 nm and 587–596 nm, respectively, in fluid solutions at 298 K (Table 3). Their emission was much less dependent on the solvent polarity and underwent a much smaller blueshift upon cooling to 77 K. These observations suggest the heavy involvement of $^3$IL (π→π*) (pq) character in the excited state. Interestingly, in aqueous buffer solution, complex **3b** exhibited a noticeably lower emission quantum yield and shorter lifetime (<1 μs) than complex **3a** and other iridium(III)–pq systems.[16a,19,21] We believe that the emissive state of complex **3b** should be mixed with some $^3$MLCT ($d$π(Ir)→π*(bpy-T)) character as a result of the electron-withdrawing triazole moiety, which stabilizes the π* orbitals of the diimine ligand.

Notably, the emission quantum yields of the diamine complexes **1a**–**4a** were considerably lower than those of their triazole counterparts **1b**–**4b** (Table 3), which is believed to be a consequence of emission quenching by the *o*-phenylenediamine moiety. Also, the emission lifetimes of the diamine complexes **1a**–**4a** were found to be dependent on the concentrations of the samples. By fitting a plot of the reciprocal value of the emission lifetime ($\tau^{-1}$) versus complex concentration [Ir], the self-quenching rate constants ($k_{sq}$) were determined to be 2.08–3.33×10$^9$ dm$^3$ mol$^{-1}$ s$^{-1}$ (after correction by diffusion limit), suggestive of a very efficient quenching process. Stern–Volmer analyses on the diamine-free control complexes [Ir-(N^C)$_2$(bpy-Me$_2$)](PF$_6$) using 2-amino-4-methoxyaniline as a quencher revealed that the biomolecular quenching rate constants ($k_q$; after correction by diffusion limit) were in the order of 10$^{10}$ dm$^3$ mol$^{-1}$ s$^{-1}$. These results illustrate that intermolecular quenching plays a key role in the self-quenching of the diamine complexes. From the first reductive potentials (−1.11 to −1.47 V versus SCE, Table 1) and the low-temperature emission energy ($E_{00}$ = 2.07–2.77 eV, Table 3) of the diamine complexes **1a**–**4a**, their excited-state reduction potentials ($E^\circ$[Ir$^{+*/0}$]) have been estimated to be ≈+0.83 to +1.37 V versus SCE. On the basis of these potentials and the irreversible first oxidation potentials (+0.41 to +0.43 V versus SCE, Table 1), the reductive quenching of the excited complexes by

| Table 3. Photophysical data of iridium(III) complexes.[a] | | | | |
|---|---|---|---|---|
| Complex | Medium (*T* [K]) | $\lambda_{em}$ [nm] | $\tau_o$ [μs] | $\Phi_{em}$ |
| **1a** | CH$_2$Cl$_2$ (298) | 522 | 1.12 | 0.028 |
| | CH$_3$CN (298) | 528 | 1.00 | 0.025 |
| | Buffer[b] (298) | 531 | 0.72 | 0.020 |
| | Glass[c] (77) | 449 (max), 482, 526 sh | 4.83 | |
| **1b** | CH$_2$Cl$_2$ (298) | 521 | 1.20 | 0.84 |
| | CH$_3$CN (298) | 530 | 1.16 | 0.66 |
| | Buffer[b] (298) | 534 | 0.84 | 0.33 |
| | Glass[c] (77) | 450, 470, 483 (max), 494 sh | 5.42 | |
| **2a** | CH$_2$Cl$_2$ (298) | 576 | 0.83 | 0.0056 |
| | CH$_3$CN (298) | 581 | 0.37 | 0.0024 |
| | Buffer[b] (298) | 582 | 0.28 | 0.0011 |
| | Glass[c] (77) | 474, 508 (max), 534 sh | 4.51 | |
| **2b** | CH$_2$Cl$_2$ (298) | 583 | 0.69 | 0.18 |
| | CH$_3$CN (298) | 590 | 0.30 | 0.070 |
| | Buffer[b] (298) | 599 | 0.12 | 0.015 |
| | Glass[c] (77) | 524, 570 sh | 4.71 | |
| **3a** | CH$_2$Cl$_2$ (298) | 552, 596 sh | 2.21 | 0.029 |
| | CH$_3$CN (298) | 556, 594 sh | 2.13 | 0.020 |
| | Buffer[b] (298) | 556, 587 sh | 2.04 | 0.013 |
| | Glass[c] (77) | 539 (max), 582, 643 sh | 4.68 | |
| **3b** | CH$_2$Cl$_2$ (298) | 554, 594 sh | 2.08 | 0.50 |
| | CH$_3$CN (298) | 556, 594 sh | 1.88 | 0.47 |
| | Buffer[b] (298) | 556, 594 sh | 0.63 | 0.14 |
| | Glass[c] (77) | 542 (max), 581, 643 sh | 4.80 | |
| **4a** | CH$_2$Cl$_2$ (298) | 623 | 1.11 | 0.024 |
| | CH$_3$CN (298) | 635 | 0.64 | 0.0022 |
| | Buffer[b] (298) | 529 | 0.83 | 0.0001 |
| | Glass[c] (77) | 599, 651 sh | 4.88 | |
| **4b** | CH$_2$Cl$_2$ (298) | 623 | 1.38 | 0.16 |
| | CH$_3$CN (298) | 634 | 0.71 | 0.070 |
| | Buffer[b] (298) | 529 sh, 653 | 0.83, 0.48 | 0.0036 |
| | Glass[c] (77) | 597, 655 sh | 4.71 | |

[a] Concentrations of the solutions were adjusted so that the absorbance at 455 nm was 0.1. [b] Potassium phosphate buffer (50 mM, pH 7.4)/MeOH (6:4, *v/v*). [c] EtOH/MeOH (4:1, *v/v*).

the diamine pendant was estimated to be favored by $\approx 0.41$–0.93 eV. Thus, photoinduced electron transfer (PeT) from the diamine pendant to the excited state is expected to occur readily, which leads to very low emission quantum yields of the complexes.

### Effects of pH value on emission properties

The change of emission properties of the diamine complex **2a** and its triazole counterpart **2b** in aerated 100 mm KCl(aq)/MeOH (6:4, *v/v*) at pH 2–12 has been studied. The pH titration curves are shown in Figure 4. Upon decreasing the pH value of the solution from pH 12, complex **2a** displayed emission enhancement at $\approx$ pH 6, and the emission intensity reached a pla-
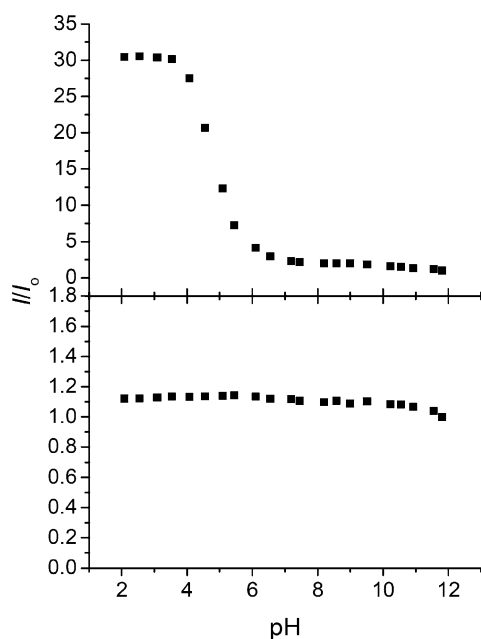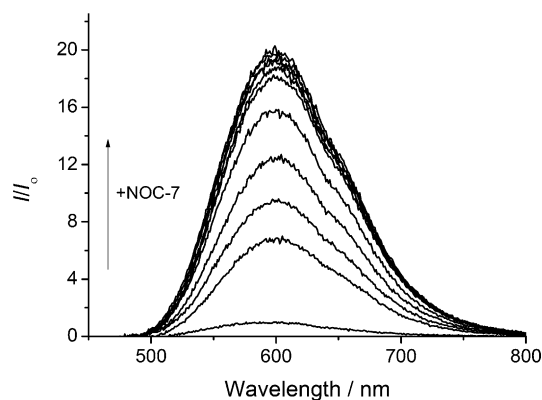
**Figure 4.** Results of the pH titrations of complexes **2a** (top) and **2b** (bottom) (5 μm) in aerated 100 mm KCl(aq)/MeOH (6:4, *v/v*) at 298 K. The emission intensity of respective complex at pH 12 was set as the reference point ($I_o$).

teau at $\approx$ pH 4, with an emission intensity gain of $\approx$ 30, whereas its triazole counterpart **2b** did not show any similar response. These findings are consistent with the suppression of PeT quenching after protonation of the *o*-phenylenediamine moiety. On the basis of the change in emission intensity, an apparent p$K$a value of $4.84 \pm 0.02$ was determined for complex **2a**, which was slightly larger than that of *o*-phenylenediamine (p$K$a$_1$ = 4.60).[23] This observation was attributed to the attachment of methoxy group, which favors the protonation of the *o*-phenylenediamine moiety. Importantly, the emission intensities of complexes **2a** and **2b** were pH insensitive in the biologically relevant pH range (pH 7.20–8.10), and that of complex **2b** was much higher than that of complex **2a** (approximately sixfold), indicating the suitability of the diamine complex **2a** to function as an intracellular NO sensor.

### NO-Sensing properties

We have examined the reactivity of the diamine complexes with NO in aqueous buffer (pH 7.4) by emission titrations using a NO-releasing agent, 3-(2-hydroxy-1-methyl-2-nitrosohydrazino)-N-methyl-1-propanamine (NOC-7; $t_{1/2}$ = 10 min, PBS buffer at pH 7.4)[24] as the titrant. Addition of NOC-7 to a solution of the diamine complex **2a** resulted in 18-fold emission enhancement at [NOC-7] = 25 μm (Figures 5 and 6), which was due to

**Figure 5.** Emission spectral traces of complex **2a** (5 μm) in aerated potassium phosphate buffer (50 mm, pH 7.4)/DMSO (99:1, *v/v*) at 298 K in the presence of NOC-7 (0–25 μm).
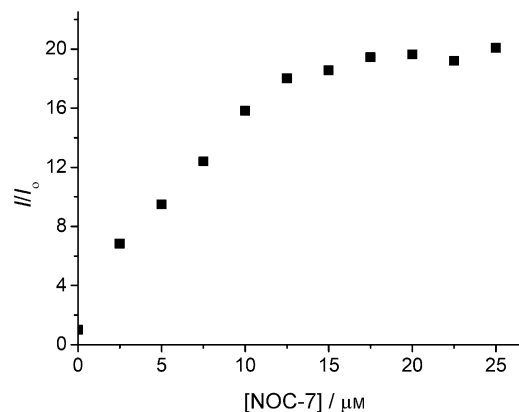
**Figure 6.** Results of the emission titration of complex **2a** (5 μm) in aerated potassium phosphate buffer (50 mm, pH 7.4)/DMSO (99:1, *v/v*) at 298 K upon addition of NOC-7.

the conversion of complex **2a** into **2b**. Similar to other diaminoaromatic compounds,[7k,l, 10–12, 15] the end point of the titration did not occur at 1:1 ratio (Figure 6), which is probably due to a complex reaction mechanism involved in the formation of the triazole derivative. The emission enhancement showed good linearity with NOC-7 concentrations ranging from 0–12.5 μm. The limit of detection (signal-to-noise ratio = 3) was estimated to be 40 nm,[7l] which is considerably higher than the ruthenium(II)- and rhenium(I)-based NO sensors.[15a,c]

In biological systems, NO is usually associated with a variety of RONS involved in different biological processes.[2b,7e,25] For

example, $O_2^-$ and $OH^•$ are usually generated concomitantly with the formation of NO. Also, NO is converted into $NO_2^-$ and $NO_3^-$ by reaction with $O_2$ and $H_2O_2$. Thus, a sensor showing high NO selectivity is imperative for its application in bioimaging. The selectivity of the diamine complex **2a** toward NO over a series of RONS has been studied. As shown in Figure 7, treat-
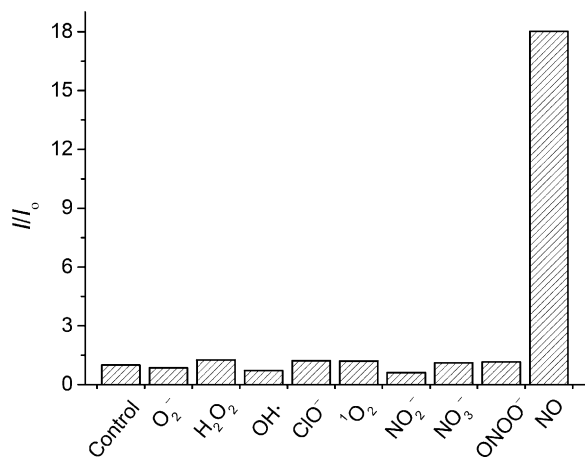


**Figure 7.** Selective emission enhancement of complex **2a** (5 μM) toward NO (25 μM) over other RONS (100 μM) in aerated potassium phosphate buffer (50 mM, pH 7.4)/DMSO (99:1, v/v) at 298 K.

ment of complex **2a** with $O_2^-$, $H_2O_2$, $OH^•$, $ClO^-$, $^1O_2$, $NO_2^-$, $NO_3^-$, or $ONOO^-$ did not induce any significant changes in the emission intensity. However, the emission intensity of a solution of complex **2a** was significantly enhanced after reaction of the complex with NO. Similar results have been observed in other diaminoaromatic-based NO sensors derived from different organic and inorganic systems,[7k,l,12a,13,15a,b,d] meaning that this selectivity for NO over other RONS originates from the diaminoaromatic unit instead of the fluorescent or phosphorescent reporting units. Overall, the physiological pH-insensitive emission properties, large emission enhancement, considerably low detection limit, and negligible interference by other biological relevant RONS strongly suggested that diamine complex **2a** can be used to detect intracellular NO under physiological conditions.

## Lipophilicity, cellular properties, and intracellular NO imaging

The lipophilicity (log $P_{o/w}$ values) of the diamine complexes **1a**–**4a** has been determined by the flask-shaking method, and the results are listed in Table 4. The lipophilicity of the complexes was found to be dependent on the hydrophobicity of the ligands; for example, the pq and pqe complexes (**3a** and **4a**) were more lipophilic than their dfppy and ppy counterparts (**1a** and **2a**). Also, the pq complex **3a** showed substantially higher lipophilicity compared to the pqe complex **4a**. Thus, the lipophilicity of complexes can be readily tuned through the introduction of a fused benzene ring or a polar substituent to the cyclometalating ligands. We were interested in the cellular properties and intracellular NO sensing ability of

**Table 4.** Lipophilicity and cellular uptake of complexes **1a**–**4a**.

| Complex | Lipophilicity (Log $P_{o/w}$)[a] | Amount of iridium [fmol][b] | Concentration of iridium [mM] |
|---|---|---|---|
| **1a** | 1.23 | 4.68 ± 0.01 | 1.37 ± 0.003 |
| **2a** | 1.35 | 4.73 ± 0.01 | 1.39 ± 0.003 |
| **3a** | 1.79 | 5.77 ± 0.03 | 1.70 ± 0.009 |
| **4a** | 1.40 | 6.67 ± 0.005 | 1.96 ± 0.001 |

[a] Log $P_{o/w}$ is defined as the logarithmic ratio of the concentration of the complex in saturated octan-1-ol with NaCl to that in an aq NaCl (0.9%, w/v). [b] Amount of iridium associated with an average HeLa cell upon incubation with the complexes (10 μM) at 37 °C for 4 h, as determined by ICP-MS.

these complexes. First, cellular uptake efficiencies of the diamine complexes **1a**–**4a** were studied by inductively coupled plasma mass spectrometry (ICP-MS) measurements using HeLa as a model cell line. Upon incubation with the complexes (10 μM) at 37 °C for 4 h, an average HeLa cell (volume = 3.4 pL) was found to contain 4.68–6.67 fmol of iridium (Table 4), which is comparable to related iridium(III) complexes such as [Ir(ppy)₂(bpyC4)](PF₆) (bpyC4 = 4,4′-bis(n-butylaminocarbonyl)-2,2′-bipyridine) (5.8 fmol of iridium),[26a] and [Ir(N^C)₂(bpy-1)](PF₆) (bpy-1 = 4,4′-ethylaminocarbonyl-2,2′-bipyridine; HN^C = Hppy or Hpq) (3.8 and 7.8 fmol of iridium, respectively).[26b] The much higher intracellular iridium concentration (1.37–1.99 mM) compared to that in the medium before uptake (10 μM) indicated efficient cellular accumulation of the complexes. Additionally, the uptake efficiency of the complexes followed the order: **1a** < **2a** < **3a** < **4a**, which is generally in accordance with their lipophilicity (Table 4). Interestingly, complex **4a** showed the most efficient uptake, although its lipophilicity was lower than that of complex **3a**. This unexpected result may be associated with the esterases in the cytoplasm, which convert the ester moieties of complex **4a** into carboxyl groups, lowering the efflux efficiency of the complex due to the negative formal charge.[13]

The cytotoxicity of the diamine complexes **1a**–**4a** toward HeLa cells has been evaluated by the MTT assay. In essence, ≈80–95% of the cells survived (Figure 8) and retained their membrane integrity after treatment with the complexes (10 μM) for 4 h, illustrating that this series of complexes does
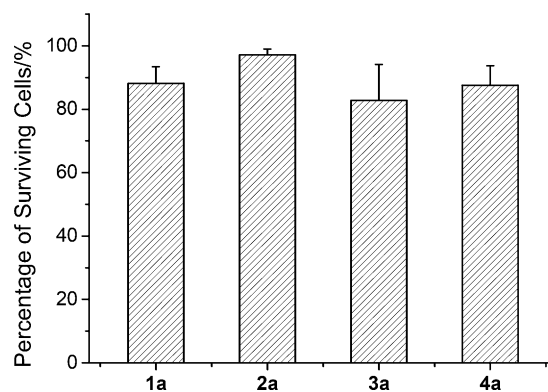


**Figure 8.** Percentage of surviving HeLa cells after exposure to complexes **1a**–**4a** (10 μM) at 37 °C for 4 h.

not have significant cytotoxic effect toward the cells. This low cytotoxic activity is also an advantage regarding the application of these complexes as intracellular sensors. The use of complex **2a**, the least cytotoxic among the four complexes, to visualize intracellular NO has been evaluated by laser-scanning confocal microscopy. HeLa cells loaded with this complex (5 μm) for 1 h displayed weak intracellular emission in the cytoplasmic region but not in the nucleus (Figure 9, left). Upon lowering the incubation temperature to 4 °C, the emission in-
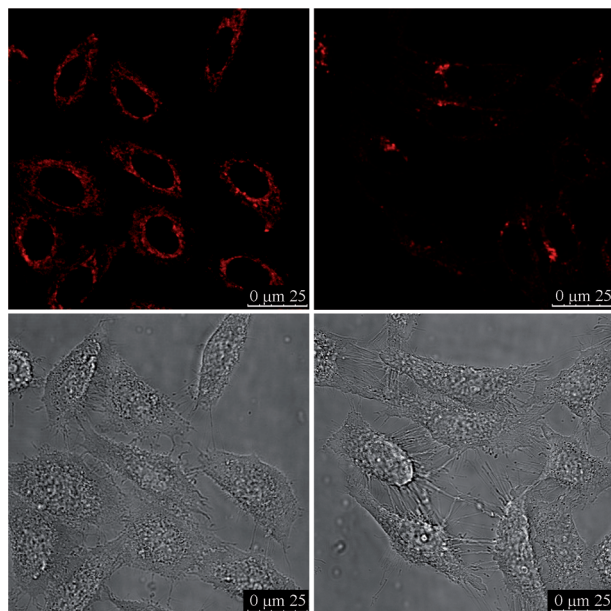


**Figure 9.** Luminescence (top) and bright-field (bottom) images of HeLa cells upon incubation with complex **2a** (5 μm) at 37 °C (left) and 4 °C (right) for 1 h, respectively.

tensity of the cells loaded with the complex was reduced significantly (Figure 9, right), implying that the internalization of the complex involved an energy-requiring pathway such as endocytosis.[27] Co-staining the cells with the complex (5 μm, 1 h) and MitoTracker Deep Red FM (100 nm, 20 min) revealed that the complex was localized in the mitochondria (Pearson's coefficient: 0.93) (Figure S1). From this result and the pH-insensitive emission of complexes **2a** and **2b** at ≈ pH 7.20–8.10 (Figure 4), we believe that the diamine complex **2a** will only be weakly emissive at the mitochondria (≈ pH 8.0) and become strongly emissive upon reaction with NO. In another experiment, when the cells were treated with the complex (5 μm, 1 h) and then incubated with NOC-7 (100 μm, 1 h) at 37 °C, the intracellular emission intensity was enhanced by approximately twofold (Figure 10). Since the ESI-MS of the cell extract revealed a peak at $m/z = 832$, corresponding to the triazole complex **2b** (Figure 11), we have confirmed that the enhanced intracellular emission originated from the conversion of the diamine complex into its triazole counterpart.

The feasibility of utilizing complex **2a** to detect intracellular NO was further tested using the macrophage cell line RAW 264.7 as a model, which is known to produce NO endogenously from iNOS in response to external endotoxins and
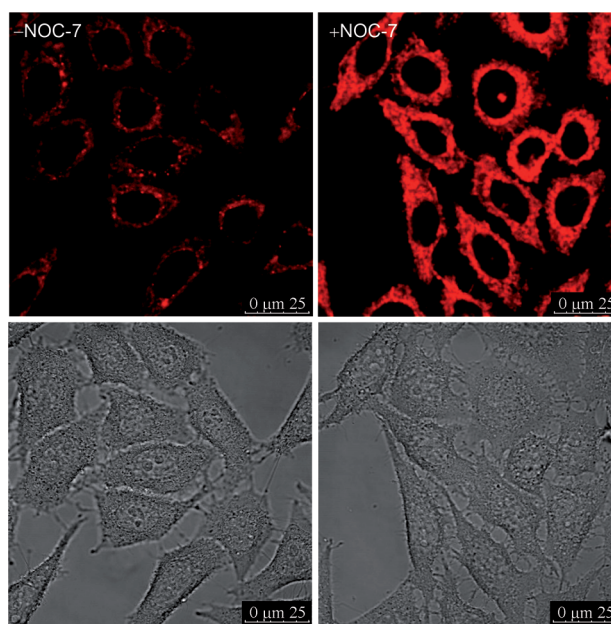


**Figure 10.** Luminescence (top) and bright-field (bottom) images of HeLa cells upon incubation with complex **2a** (5 μm, 1 h) at 37 °C without (left) and with (right) posttreatment with NOC-7 (100 μm, 1 h)
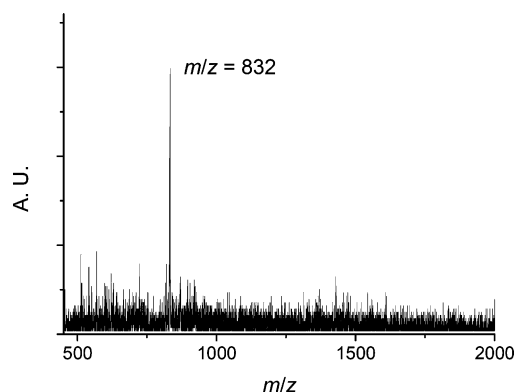


**Figure 11.** ESI mass spectrum of the product extracted from HeLa cells treated with complex **2a** (5 μm, 1 h), followed by washing and incubation with NOC-7 (100 μm, 1 h) at 37 °C.
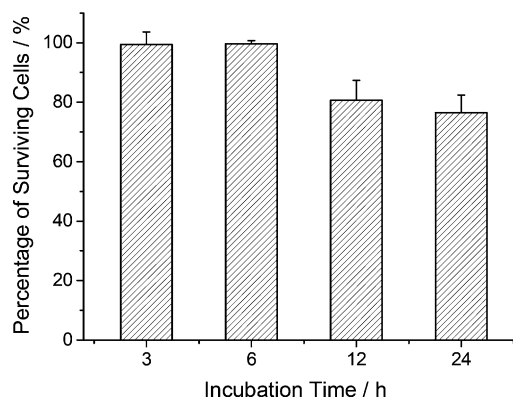


**Figure 12.** Percentage of surviving RAW 264.7 murine macrophages after exposure to complex **2a** (5 μm) at 37 °C.
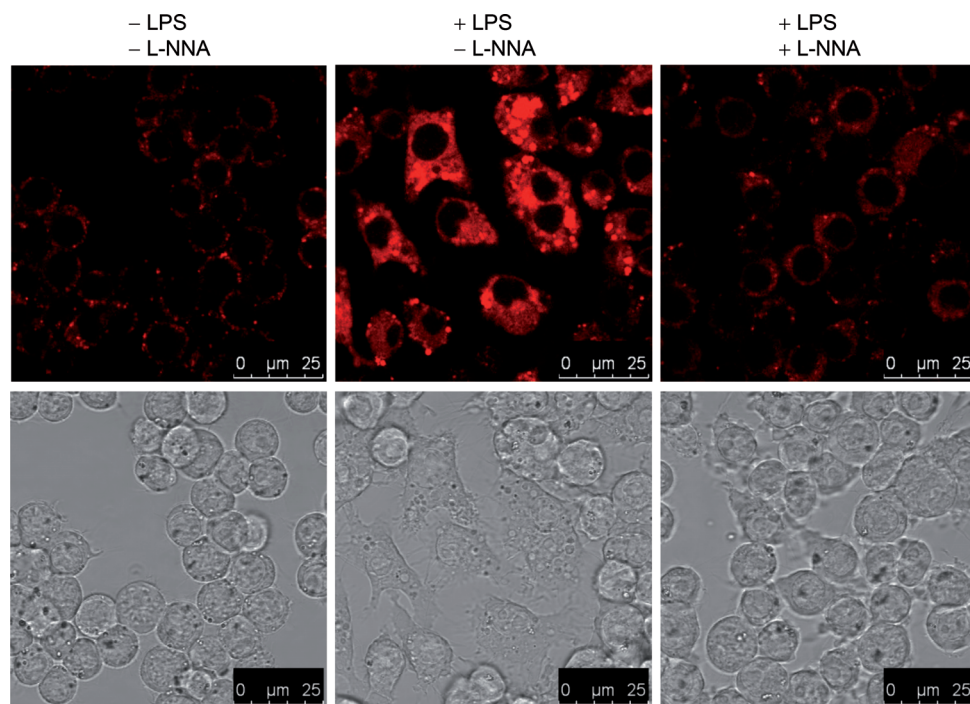
**Figure 13.** Luminescence (top) and bright-field (bottom) images of RAW 264.7 murine macrophages upon incubation with complex **2a** (5 μM) at 37 °C for 1 h without pretreatment (left), pretreated with LPS (1 μg mL$^{-1}$, 18 h) only (middle), and pretreated simultaneously with both LPS (1 μg mL$^{-1}$, 18 h) and L-NNA (1 mM, 18 h) (right).

cytokines such as lipopolysaccharides (LPS) and interferon-γ stimulation.[28] MTT results showed that ≈98% of the cells survived after being treated with complex **2a** (5 μM) for 3–6 h (Figure 12). When the incubation time was extended to 12–24 h, the percentage of surviving cells moderately decreased to ≈80%, reflecting the low cytotoxic activity of this complex toward RAW 264.7. The emission intensity of the cells stimulated with LPS (1 μg mL$^{-1}$) for 18 h prior to addition of complex **2a** has been investigated by laser-scanning confocal microscopy. Without the addition of LPS, cells that were stained with complex **2a** only displayed weak emission (Figure 13, left). In contrast, pretreatment of the cells with LPS resulted in ≈3.7-fold emission intensity enhancement (Figure 13, middle). However, when the cells were simultaneously pretreated with LPS (1 μg mL$^{-1}$) and $N_\omega$-nitro-L-arginine (L-NNA), an iNOS inhibitor with a $K_i$ value of 4.4 μM for murine macrophages (1 mM),[29] the emission intensity of the cells remained very low (Figure 13, right), indicative of the inhibition of intracellular NO production. All these findings have established that complex **2a** is capable of detecting endogenous levels of NO.

## Conclusions

In this work, a novel class of phosphorescent cyclometalated iridium(III) bipyridyl–phenylenediamine complexes were synthesized; their electrochemical, photophysical, lipophilicity, cellular uptake efficiency, and cytotoxic characteristics were investigated. Results from a range of experiments demonstrated that the emission of the diamine complex **2a** was pH insensitive in the biologically relevant range (≈pH 7.20–8.10). The

complex was highly reactive toward NO over other RONS, with the formation of triazole complex **2b** that showed much higher emission intensity. Inductively coupled plasma mass spectrometry (ICP-MS) analyses and cell viability experiments indicated that all of the diamine complexes were effectively internalized into the cells and their cytotoxic effects were negligible. Laser-scanning confocal images revealed that complex **2a** was preferentially localized in the mitochondria of HeLa cells with very weak emission intensity. Also, the internalization of this complex involved an energy-requiring pathway. Importantly, confocal microscopy experiments involving cultured HeLa cells and RAW 264.7 murine macrophages showed that complex **2a** was capable of reacting with exogenous and endogenous NO, respectively. The formation of triazole complex **2b** led to significant intracellular emission enhancement. We anticipate that this class of iridium-(III) bipyridyl–phenylenediamine complexes will be useful for phosphorescence detection of NO in biological systems.

## Experimental Section

### Materials

All solvents were of analytical grade and purified according to standard procedures.[30] All buffer components were of biological grade and used as received. 4,4′-Dimethyl-2,2′-bipyridine, SeO$_2$, IrCl$_3$·3H$_2$O, 2-(2,4-difluorophenyl)pyridine (Hdfppy), 2-phenylpyridine (Hppy), 2-phenylquinoline (Hpq), 2-phenyl-4-quinolinecarboxylic acid, sodium metabisulfite, and di-*tert*-butyl dicarbonate, tetra-*n*-butylammonium hexafluorophosphate (TBAP), KOH, and 10% Pd/C were obtained from Aldrich. NaH in mineral oil (60%, *w/w*), 4-amino-3-nitrophenol, NaHCO$_3$, sodium cyanoborohydride (1.0 M solution in THF), trifluoroacetic acid (TFA), CH$_3$I, KPF$_6$, NaCl, H$_2$O$_2$, ferrocene, NaOH, NaClO, NaNO$_2$, NaNO$_3$, ammonium iron(II) sulfate hexahydrate, octan-1-ol, and KO$_2$ were obtained from Acros. 3-(4,5-Dimethyl-2-thiazolyl)-2,5-diphenyltetrazolium bromide (MTT), lipopolysaccharides (LPS), and $N_\omega$-nitro-L-arginine (L-NNA) were purchased from Sigma. All chemicals were used without further purification except that TBAP was recrystallized from hot EtOH and dried in vacuo at 110 °C before use. Iridium dimers [Ir$_2$(N^C)$_4$Cl$_2$] (HN^C = Hdfppy, Hppy, Hpq), Hpqe, and bpy-CHO were prepared as previously reported.[16d,31] Autoclaved Milli-Q H$_2$O was used for the preparation of aqueous buffer solutions. Reagent 3-(2-hydroxy-1-methyl-2-nitrosohydrazino)-*N*-methyl-1-propanamine (NOC-7) and sodium peroxynitrite were purchased from Calbiochem. HeLa cells and RAW 264.7 murine macrophages were obtained from American Type Culture Collection (ATCC). High glucose Dulbecco's

modified Eagle's medium (DMEM), fetal bovine serum (FBS), phosphate-buffered saline (PBS), trypsin-EDTA, penicillin/streptomycin, and MitoTracker Deep Red FM were purchased from Invitrogen.

### Synthesis

**4-Methoxy-2-nitroanline**: NaH (270 mg, 6.60 mmol, 60% in mineral oil) was added to a solution of 4-amino-3-nitrophenol (1.0 g, 6.51 mmol) in dry *N,N*-dimethylformamide (DMF; 25 mL) at 0 °C under an inert atmosphere of $N_2$. After the mixture was stirred for 30 min, it was slowly warmed to RT, and $CH_3I$ (420 µL, 6.60 mmol) was added slowly. The mixture was stirred for 24 h, and cold $H_2O$ (5 mL) was added to quench the reaction. The solvent was removed by evaporation in vacuo. The crude product was purified by column chromatography on silica gel using *n*-hexane/EtOAc (4:1, *v/v*) as the eluent. The product was subsequently isolated as a red solid (1.02 g, 90%): ^{1}H NMR (400 MHz, CDCl3, 298 K, TMS): $\delta =$ 7.54 (d, *J* = 2.8 Hz, 1 H, *H3*), 7.07 (dd, *J* = 9.2, 2.8 Hz, 1 H, *H5*), 6.77 (d, *J* = 9.2 Hz, 1 H, *H6*), 5.94 (br s, 2 H, *NH₂*), 3.79 ppm (s, 3 H, *OCH₃*); MS (ESI[+]): *m/z* (%): 169 (100) [*M*+H][+].

**N-(tert-Butoxycarbonyl)-4-methoxy-2-nitroanaline**: NaH (1.56 g, 39.0 mmol, 60% in mineral oil) was added to a solution of 4-methoxy-2-nitroaniline (936 mg, 5.57 mmol) in dry THF (30 mL) at 0 °C under an inert atmosphere of nitrogen. After the mixture was stirred for 30 min, a THF solution of (Boc)₂O (1.46 g, 6.68 mmol, 20 mL) was added slowly at RT, and the mixture was stirred for 24 h. After quenching with cold $H_2O$ (10 mL), the mixture was extracted with EtOAc (40 mL×3). The organic solution was washed with saturated aq NaHCO₃ (50 mL) and saturated aq NaCl (50 mL), and dried over MgSO₄. The solvent was removed by evaporation in vacuo, and the resultant solid was purified by column chromatography on silica gel using *n*-hexane/EtOAc (15:1, *v/v*) as the eluent. The product was subsequently isolated as an orange solid (1.30 g, 87%): ^{1}H NMR (400 MHz, CDCl3, 298 K, TMS): $\delta =$ 9.28 (s, 1 H, *NH*), 8.27 (d, *J* = 9.6 Hz, 1 H, *H6*), 7.45 (d, *J* = 2.8 Hz, 1 H, *H3*), 7.04 (dd, *J* = 9.2, 3.2 Hz, 1 H, *H5*), 3.72, (s, 3 H, *OCH₃*), 1.44 ppm (s, 9 H, CH₃ of Boc); MS (ESI[+]): *m/z* (%): 291 (100) [*M*+Na][+].

**2-(N-tert-Butoxycarbonylamino)-5-methoxyaniline**: A mixture of *N*-(*tert*-butoxycarbonyl)-4-methoxy-2-nitroanaline (1.30 g, 4.85 mmol) and 10% Pd/C (130 mg) in MeOH (40 mL) was stirred under hydrogen atmosphere at ambient balloon pressure for 24 h. The residue was filtered, and the solvent was evaporated to dryness to yield a grey solid (1.10 g, 95%): ^{1}H NMR (300 MHz, CDCl3, 298 K, TMS): $\delta =$ 7.05 (d, *J* = 9.3 Hz, 1 H, *H3*), 6.34–6.31 (m, 2 H, *H4* and *H6*), 6.01 (br s, 1 H, N*H*(Boc)), 3.84 (br s, 2 H, *NH₂*), 3.75 (s, 3 H, *OCH₃*), 1.50 ppm (s, 9 H, CH₃ of Boc); MS (ESI[+]): *m/z* (%): 477 (100) [*M*×2+H][+].

**4-(N-(2-(N-tert-Butoxycarbonylamino)-5-methoxyphenyl)amino-methyl)-4′-methyl-2,2′-bipyridine (bpy-DA-Boc)**: A mixture of 2-(*N*-*tert*-butoxycarbonylamino)-5-methoxyaniline (1.11 g, 4.64 mmol) and bpy-CHO (920 mg, 4.64 mmol) in $CH_2Cl_2$ (30 mL) was slowly added with acetic acid (531 µL, 9.28 mol), and stirred for 2 h. Sodium cyanoborohydride (4.64 mL, 4.64 mmol, 1.0 M in THF) was then added slowly at 0 °C, and the reaction mixture was stirred for another 2 h. After quenching with cold $H_2O$ (6 mL), the reaction mixture was extracted with $CH_2Cl_2$ (2×100 mL). The combined organic layer was washed with saturated aq NaCl (50 mL) and dried over MgSO₄. The solvent was evaporated to dryness, and the residue was further purified by column chromatography on silica gel using *n*-hexane/EtOAc/NH₄OH (2:1:0.1, *v/v/v*) as the eluent. A pale pink solid was obtained after the solvent was removed (1.08 g, 56%): ^{1}H NMR (300 MHz, CDCl3, 298 K, TMS): $\delta =$ 8.54 (d, *J* = 4.5 Hz,

1 H, *H6* of bpy), 8.48 (d, *J* = 5.1 Hz, 1 H, *H6′* of bpy), 8.30 (s, 1 H, *H3* of bpy), 8.16 (s, 1 H, *H3′* of bpy), 7.24 (d, *J* = 5.1 Hz, 1 H, *H5* of bpy), 7.09–7.04 (m, 2 H, *H5′* of bpy and *H3* of phenyl ring), 6.38 (br s, 1 H, N*H*(Boc)), 6.19 (dd, *J* = 8.7, 2.1 Hz, 1 H, *H4* of phenyl ring), 6.01 (d, *J* = 2.1 Hz, 1 H, *H6* of phenyl ring), 4.85 (br, 1 H, CH₂N*H*), 4.30 (s, 2 H, C*H₂*NH), 3.61 (s, 3 H, *OCH₃*), 2.36 (s, CH₃ of bpy), 1.44 ppm (s, 9 H, CH₃ of Boc); ^{13}C NMR (100 MHz, CDCl3, 298 K, TMS): $\delta =$ 21.2, 28.3, 47.0, 55.3, 80.5, 101.8, 116.7, 119.6, 122.0, 122.1, 124.8, 144.1, 148.2, 148.9, 149.6, 149.7, 155.8, 156.5, 159.2 ppm; MS (ESI[+]): *m/z* (%): 421 (100) [*M*+H][+].

**[Ir(dfppy)₂(bpy-DA-Boc)](PF₆)**: A mixture of [Ir₂(dfppy)₄Cl₂] (286 mg, 0.23 mmol) and bpy-DA-Boc (198 mg, 0.47 mmol) in $CH_2Cl_2$/MeOH (40 mL, 1:1, *v/v*) was heated to reflux under an inert atmosphere of nitrogen in the dark for 24 h. The reaction mixture was cooled to RT and stirred for 30 min after addition of KPF₆ (47.5 mg, 0.26 mmol). The solvent was evaporated to dryness, and the obtained solid was purified by column chromatography on silica gel using *n*-hexane/EtOAc (1:1, *v/v*) as the eluent. Subsequent recrystallization of the solid from $CH_2Cl_2$/Et₂O afforded the complex as yellow-orange crystals (275 mg, 51%): ^{1}H NMR (300 MHz, [D₄]methanol, 298 K, TMS): $\delta =$ 8.73 (s, 1 H, *H3* of bpy), 8.64 (s, 1 H, *H3′* of bpy), 8.33 (d, *J* = 8.4 Hz, 2 H, *H6* pyridyl ring of dfppy), 7.94–7.87 (m, 3 H, *H5* of pyridyl ring of dfppy, *H6* and *H6′* of bpy), 7.67–7.57 (m, 3 H, *H3* of pyridyl ring of dfppy and *H5* of bpy), 7.39 (d, *J* = 7.6 Hz, 1 H, *H5′* of bpy), 7.10 (t, *J* = 7.6 Hz, 2 H, *H4* of pyridyl ring of dfppy), 6.95 (d, *J* = 8.4 Hz, 1 H, *H3* of phenyl ring of bpy-DA-Boc), 6.69–6.61 (m, 2 H, *H6* of phenyl ring of dfppy), 6.16 (dd, *J* = 8.4, 2.4 Hz, 1 H, *H4* of phenyl ring of bpy-DA-Boc), 5.89 (s, 1 H, *H6* of phenyl ring of bpy-DA-Boc), 5.71–5.68 (m, 2 H, *H4* of phenyl ring of dfppy), 4.65 (s, 2 H, C*H₂*NH), 3.54 (s, 3 H, *OCH₃*), 2.55 (s, 3 H, CH₃ of bpy), 1.53 ppm (s, 9 H, CH₃ of Boc); MS (ESI[+]): *m/z* (%): 993 (100) [*M*−PF₆^{−}][+].

**[Ir(ppy)₂(bpy-DA-Boc)](PF₆)**: The synthetic procedure was performed as described for [Ir(pq)₂(bpy-DA-Boc)](PF₆); however, [Ir₂(ppy)₄Cl₂] (320 mg, 0.30 mmol) was used instead of [Ir₂(dfppy)₄Cl₂]. The crude product was purified by column chromatography on silica gel using $CH_2Cl_2$/MeOH (50:1, *v/v*) as the eluent and subsequently recrystallized from $CH_2Cl_2$/Et₂O afforded the complex as yellow crystals (560 mg, 89%): ^{1}H NMR (300 MHz, [D₄]methanol, 298 K, TMS): $\delta =$ 8.69 (s, 1 H, *H3* of bpy), 8.59 (s, 1 H, *H3′* of bpy), 8.09 (d, *J* = 8.1 Hz, 2 H, *H3* of pyridyl ring of ppy), 7.86–7.81 (m, 6 H, *H5* and *H6* of bpy, *H4* of pyridyl ring and *H3* of phenyl ring of ppy), 7.60–7.50 (m, 3 H, *H5′* of bpy and *H6* of pyridyl ring of ppy), 7.33 (s, 1 H, *H6′* of bpy), 7.02–6.94 (m, 5 H, *H4* of phenyl ring, *H5* of pyridyl ring of ppy, *H3* of phenyl ring of bpy-DA-Boc), 6.88–6.86 (m, 2 H, *H5* of phenyl ring of ppy), 6.28 (d, *J* = 7.2 Hz, 2 H, *H6* of phenyl ring of ppy), 6.18 (d, *J* = 9.3 Hz, *H4* of phenyl ring of bpy-DA-Boc), 5.89 (s, 1 H, *H6* of phenyl ring of bpy-DA-Boc), 4.61 (s, 2 H, C*H₂*NH), 3.56 (s, 3 H, *OCH₃*), 2.54 (s, 3 H, CH₃ of bpy), 1.53 ppm (s, 9 H, CH₃ of Boc); MS (ESI[+]): *m/z* (%): 922 (100) [*M*−PF₆^{−}][+].

**[Ir(pq)₂(bpy-DA-Boc)](PF₆)**: The synthetic procedure was performed as described for [Ir(ppy)₂(bpy-DA-Boc)](PF₆); however, [Ir₂(pq)₄Cl₂] (200 mg, 0.16 mmol) was used instead of [Ir₂(ppy)₄Cl₂]. The solvent was evaporated to dryness, and the resultant solid was purified by column chromatography on silica gel using *n*-hexane/EtOAc (1:1, *v/v*) as the eluent. Subsequent recrystallization of the solid from $CH_2Cl_2$/Et₂O afforded the complex as orange crystals (220 mg, 59%): ^{1}H NMR (400 MHz, [D₄]methanol, 298 K, TMS): $\delta =$ 8.39–8.31 (m, 5 H, H3 of quinoline and *H3* of phenyl ring of pq, *H3* of bpy), 8.18–8.10 (m, 4 H, *H4* of quinoline of pq, *H3′* and *H6* of bpy), 8.04 (d, *J* = 5.6 Hz, 1 H, *H6′* of bpy), 7.84–7.78 (m, 2 H, *H8* of quinoline of pq), 7.52 (d, *J* = 6.0 Hz, 1 H, *H5* of bpy), 7.43–7.33 (m,

4H, *H5* and *H7* of quinoline of pq), 7.21–7.14 (m, 3H, *H5'* of bpy and *H4* of phenyl ring of pq), 7.02–6.93 (m, 3H, *H3* of phenyl ring of bpy-DA-Boc and *H6* of quinoline of pq), 6.79 (t, *J*=7.5 Hz, 2H, *H5* of phenyl ring of pq), 6.52–6.49 (m, 2H, *H6* of phenyl ring of pq), 6.21 (dd, *J*=8.4, 2.8 Hz, 1H, *H4* of phenyl ring of bpy-DA-Boc), 5.76 (d, *J*=2.4 Hz, 1H, *H6* of phenyl ring of bpy-DA-Boc), 4.51 (s, 2H, *CH₂NH*), 3.63 (s, 3H, *OCH₃*), 2.42 (s, 3H, *CH₃* of bpy), 1.49 ppm (s, 9H, *CH₃* of Boc); MS (ESI⁺): *m/z* (%): 1022 (100) [*M*−PF₆⁻]⁺.

**[Ir(pqe)₂(bpy-DA-Boc)](PF₆)**: The synthetic procedure was performed as described for [Ir(ppy)₂(bpy-DA-Boc)](PF₆); however, [Ir₂(pqe)₄Cl₂] (499 mg, 0.33 mmol) was used instead of [Ir₂(pq)₄Cl₂]. The crude product was purified by column chromatography on silica gel using *n*-hexane/EtOAc (1:2, *v/v*) as the eluent and subsequently recrystallized from CH₂Cl₂/Et₂O to afford the complex as deep red crystals (404 mg, 95%): ¹H NMR (400 MHz, [D₄]methanol, 298 K, TMS): δ=8.78 (s, 1H, *H3* of quinoline of pqe), 8.74 (s, 1H, *H3* of quinoline of pqe), 8.54 (d, *J*=8.6 Hz, *H5* of quinoline of pqe), 8.49 (d, *J*=8.8 Hz, 1H, *H5* of quinoline of pqe), 8.31 (s, 1H, *H3* of bpy), 8.24–8.18 (m, 3H, *H3* of phenyl ring of pqe, *H3'* of bpy), 8.08 (d, *J*=6.0 Hz, 1H, *H6* of bpy), 8.02 (d, *J*=6.0 Hz, 1H, *H6'* of bpy), 7.59–7.57 (m, 2H, *H8* of quinoline of pqe, *H5* of bpy), 7.47–7.34 (m, 4H, *H6* and *H8* of quinoline of pqe, *H5'* of bpy), 7.20 (t, *J*=7.6 Hz, 1H, *H4* of phenyl of pqe), 6.86–6.82 (m, 1H, *H7* of quinoline of pqe), 6.96–6.92 (m, 1H, *H7* of quinoline of pqe, *H3* of phenyl ring of bpy-DA-Boc), 6.84 (t, *J*=7.6 Hz, 2H, *H5* of phenyl ring of pqe), 6.55 (dd, *J*=7.2, 2.4 Hz, 2H, *H6* of phenyl ring of pqe), 6.19 (dd, *J*=8.4, 2.4 Hz, 1H, *H4* of phenyl ring of bpy-DA-Boc), 5.75 (d, *J*=2.8 Hz, 1H, *H6* of phenyl ring of bpy-DA-Boc), 4.51 (s, 2H, *CH₂NH*), 4.13 (s, 3H, *CO₂CH₃*), 4.11(s, 3H, *CO₂CH₃*), 3.60 (s, 3H, *OCH₃*), 2.42 (s, 3H, *CH₃* of bpy), 1.48 ppm (s, 9H, *CH₃* of Boc); MS (ESI⁺): *m/z* (%): 1137 (100) [*M*−PF₆⁻]⁺.

**[Ir(dfppy)₂(bpy-DA)](PF₆) (1 a)**: TFA (1 mL) was slowly added to a CH₂Cl₂ solution (10 mL) of [Ir(dfppy)₂(bpy-DA-Boc)](PF₆) (196 mg, 0.17 mmol), and the resultant mixture was stirred in the dark for 2 h. The solution was neutralized by addition of NH₄OH. The mixture was extracted with CH₂Cl₂ (2×100 mL). The combined organic layer was washed with saturated aq NaCl (50 mL), dried over MgSO₄, and evaporated to dryness. The residual solid was dissolved in CH₂Cl₂/MeOH (30 mL, 1:1, *v/v*) containing KPF₆ (34.9 mg, 0.19 mmol) and stirred for 2 h. The solvent was removed in vacuo and the solid was recrystallized from CH₂Cl₂/Et₂O yielding complex **1 a** as light brown crystals (146 mg, 82%): ¹H NMR (400 MHz, [D₄]methanol, 298 K, TMS): δ=8.71 (s, 1H, *H3* of bpy), 8.59 (s, 1H, *H3'* of bpy), 8.36 (d, *J*=8.7 Hz, 2H, *H6* of pyridyl ring of dfppy), 7.98–7.91 (m, 3H, *H5* of pyridyl ring of dfppy and *H6* of bpy), 7.84 (d, *J*=5.1 Hz, 1H, *H6'* of bpy), 7.68–7.62 (m, 3H, *H3* of pyridyl ring of dfppy, *H5* of bpy), 7.44 (d, *J*=5.1 Hz, 1H, *H5'* of bpy), 7.14–7.10 (m, 2H, *H4* of pyridyl ring of dfppy), 6.73–6.65 (m, 3H, *H3* of phenyl ring of bpy-DA, *H6* of phenyl ring of dfppy), 6.15 (dd, *J*=8.4, 2.7 Hz, 1H, *H4* of phenyl ring of bpy-DA), 5.90 (d, *J*=2.7 Hz, 1H, *H6* of phenyl ring of bpy-DA), 5.72–5.68 (m, 2H, *H4* of phenyl ring of dfppy), 4.63, (s, 2H, *CH₂NH*), 3.50 (s, 3H, *OCH₃*), 2.58 ppm (s, 3H, *CH₃* of bpy); ¹³C NMR (100 MHz, [D₆]DMSO, 298 K, TMS): δ= 21.4, 46.3, 55.4, 98.9, 99.4, 101.5, 113.6, 123.7, 123.9, 124.1, 124.9, 126.32, 127.7, 128.0, 130.1, 140.5, 149.8, 149.9, 150.5, 152.7, 155.2, 155.3, 155.4, 155.5, 159.9, 162.1, 163.2, 163.3, 164.5 ppm; IR (KBr): *ṽ*=3423 cm⁻¹ (N−H), 845 (PF₆⁻); MS (ESI⁺): *m/z* (%): 894 (100) [*M*−PF₆⁻]⁺; Anal. calcd for IrC₄₁H₃₂N₆OPF₁₀·CH₃OH: C 47.15, H 3.39, N 7.85, found: C 47.38, H 3.63, N 7.72.

**[Ir(ppy)₂(bpy-DA)](PF₆) (2 a)**: The synthetic procedure was performed as described for complex **1 a**; however, [Ir(ppy)₂(bpy-DA-Boc)](PF₆) (210 mg, 0.20 mmol) was used instead of [Ir(dfppy)₂(bpy-

DA-Boc)](PF₆). Complex **2 a** was isolated as brown crystals (170 mg, 88%): ¹H NMR (400 MHz, [D₄]methanol, 298 K, TMS): δ=8.68 (s, 1H, *H3* of bpy), 8.54 (s, 1H, *H3'* of bpy), 8.12 (d, *J*=8,4 Hz, 2H, *H3* of pyridyl ring of ppy), 7.92–7.81 (m, 6H, *H5* and *H6* of bpy, *H4* of pyridyl ring, *H3* of phenyl ring of ppy), 7.63 (d, *J*=5.6 Hz, 1H, *H5'* of bpy), 7.59–7.55 (m, 2H, *H6* of pyridyl ring of ppy), 7.37 (d, *J*=5.6 Hz, 1H, *H6'* of bpy), 7.07–7.00 (m, 4H, *H5* of pyridyl ring, *H4* of phenyl ring of ppy), 6.88 (t, *J*=7.2 Hz, 2H, *H5* of phenyl ring of ppy), 6.72 (d, *J*=8.4 Hz, 1H, *H3* of phenyl ring of bpy-DA), 6.29 (d, *J*=7.6 Hz, 2H, *H6* of phenyl ring of ppy), 6.16 (dd, *J*=8.4, 2.4 Hz, 1H, *H4* of phenyl ring of bpy-DA), 5.93 (d, *J*=2.4 Hz, 1H, *H6* of phenyl ring of bpy-DA), 4.61 (s, 2H, *CH₂NH*), 3.56 (s, 3H, *OCH₃*), 2.57 ppm (s, 3H, *CH₃* of bpy); ¹³C NMR (100 MHz, [D₆]DMSO, 298 K, TMS): δ=21.4, 46.6, 55.4, 98.9, 101.6, 115.7, 120.5, 122.6, 123.9, 124.2, 124.3, 125.5, 126.0, 127.3, 129.6, 129.8, 130.7, 131.5, 137.2, 139.2, 144.2, 149.0, 149.2, 149.6, 150.0, 151.1, 152.0, 153.0, 154.9, 155.4, 155.7, 167.3, 167.4 ppm; IR (KBr): *ṽ*=3421 (N−H), 843 (PF₆⁻) cm⁻¹; MS (ESI⁺): *m/z* (%): 822 (100) [*M*−PF₆⁻]⁺; Anal. calcd for IrC₄₁H₃₆N₆OPF₆·0.5(CH₃CH₂)₂O: C 51.49, H 4.12, N 8.38, found: C 51.39, H 4.10, N 8.52.

**[Ir(pq)₂(bpy-DA)](PF₆) (3 a)**: The synthetic procedure was performed as described for complex **1 a**; however, [Ir(pq)₂(bpy-DA-Boc)](PF₆) (190 mg, 0.17 mmol) was used instead of [Ir(dfppy)₂(bpy-DA-Boc)](PF₆). Complex **3 a** was isolated as reddish brown crystals (130 mg, 75%): ¹H NMR (300 MHz, [D₄]methanol, 298 K, TMS): δ= 8.35 (d, *J*=4.8 Hz, 4H, *H3* of quinoline and *H3* of phenyl ring of pq), 8.28 (s, 1H, *H3* of bpy), 8.15–8.08 (m, 4H, H4 of quinoline of pq, *H3'* and *H6* of bpy), 8.03 (d, *J*=5.7 Hz, 1H, *H6'* of bpy), 7.81–7.76 (m, 2H, *H8* of quinoline of pq), 7.52 (d, *J*=5.4 Hz, 1H, *H5* of bpy), 7.42–7.28 (m, 4H, *H5* and *H7* of quinoline of pq), 7.21 (d, *J*=9.0 Hz, 1H, *H5'* of bpy), 7.15–7.10 (m, 2H, *H4* of phenyl ring of pq), 7.04–6.86 (m, 2H, *H6* of quinoline of pq), 6.78–6.78 (m, 2H, *H5* of phenyl ring of pq), 6.68 (d, *J*=8.7 Hz, *H3* of phenyl ring of bpy-DA), 6.49 (d, *J*=8.1 Hz, 2H, *H6* of phenyl ring of pq), 6.15 (dd, *J*=8.1, 2.4 Hz, 1H, *H4* of phenyl ring of bpy-DA), 5.74 (d, *J*=2.7 Hz, 1H, *H6* of phenyl ring of bpy-DA), 4.46 (s, 2H, *CH₂NH*), 3.56 (s, 3H, *OCH₃*), 2.40 ppm (s, 3H, *CH₃* of bpy); ¹³C NMR (100 MHz, [D₆]DMSO, 298 K, TMS): δ=21.2, 55.3, 98.9, 101.1, 115.71, 118.7, 123.1, 124.3, 124.6, 125.1, 127.2, 127.9, 128.2, 129.6, 129.8, 131.0, 134.1, 136.8, 140.8, 146.2, 146.3, 147.1, 147.4, 151.7, 152.1, 152.9, 155.0, 155.2, 155.3, 170.2, 170.3 ppm; IR (KBr): *ṽ*=3448 cm⁻¹ (N−H), 845 (PF₆⁻); MS (ESI⁺): *m/z* (%): 922 (100) [*M*−PF₆⁻]⁺; Anal. calcd for IrC₄₉H₄₀N₆OPF₆·H₂O·(CH₃CH₂)₂O: C 54.96, H 4.53, N 7.26, found: C 54.97, H 4.57, N 7.45.

**[Ir(pqe)₂(bpy-DA)](PF₆) (4 a)**: The synthetic procedure was performed as described for complex **1 a**; however, [Ir(pqe)₂(bpy-DA-Boc)](PF₆) (404 mg, 0.32 mmol) was used instead of [Ir(dfppy)₂(bpy-DA-Boc)](PF₆). Complex **4 a** was isolated as a brown solid (334 mg, 90%): ¹H NMR (400 MHz, [D₄]methanol, 298 K, TMS): δ=8.87 (s, 1H, *H3* of quinoline of pqe), 8.74 (s, 1H, *H3* of quinoline of pqe), 8.55 (d, *J*=8.4 Hz, 1H, *H5* of quinoline of pqe), 8.49 (d, *J*=8.4 Hz, 1H, *H5* of quinoline of pqe), 8.30 (s, 1H, *H3* of bpy), 8.23 (t, *J*=6.8 Hz, *H3* of phenyl ring of pqe), 8.13 (s, 1H, *H3'* of bpy), 8.09 (d, *J*=5.6 Hz, 1H, *H6* of bpy), 8.04 (d, *J*=5.6 Hz, 1H, *H6'* of bpy), 7.60–7.58 (m, 2H, *H8* of quinoline of pqe, *H5* of bpy), 7.48–7.34 (m, 4H, *H6* and *H8* of quinoline of pqe, H5' of bpy), 7.12 (t, *J*=7.2 Hz, 2H, *H4* of phenyl ring of pqe), 7.10–7.06 (m, 1H, *H7* of quinoline of pqe), 6.93–6.83 (m, 3H, *H7* of quinolone, *H5* of phenyl ring of pqe), 6.69 (d, *J*=8.4 Hz, 1H, *H3* of phenyl ring of bpy-DA), 6.55 (d, *J*=7.6 Hz, 2H, *H6* of phenyl ring of pqe), 6.15 (dd, *J*=8.4, 2.4 Hz, 1H, *H4* of phenyl ring of bpy-DA), 5.76 (d, *J*=2.8 Hz, 1H, *H6* of phenyl ring of bpy-DA), 4.49 (s, 2H, *CH₂NH*), 4.13 (s, 3H, *CO₂CH₃*), 4.12 (s,

3H, CO$_2$C$H_3$), 3.56 (s, 3H, OC$H_3$), 2.43 ppm (s, 3H, C$H_3$ of bpy); $^{13}$C NMR (100 MHz, [D$_6$]DMSO, 298 K, TMS): $\delta$ = 21.2, 46.1, 53.8, 53.9, 55.3, 99.0, 101.1, 115.7, 119.1, 123.9, 124.0, 126.9, 128.8, 129.6, 129.8, 131.8, 134.5, 136.8, 139.4, 139.5, 145.6, 145.7, 147.7, 147.9, 151.8, 152.4, 152.9, 154.7, 155.0, 155.7, 165.7, 170.1, 170.2 ppm; IR (KBr): $\tilde{v}$ = 3418 (N—H), 1728 cm$^{-1}$ (C=O), 844 (PF$_6^-$); MS (ESI$^+$): m/z (%): 1037 (100) [M−PF$_6^-$]$^+$; Anal. calcd for IrC$_{53}$H$_{44}$N$_6$O$_5$PF$_6$·CH$_3$OH: C 53.42, H 3.98, N 6.92, found: C 53.61, H 3.68, N 6.69.

**[Ir(dfppy)$_2$(bpy-T)](PF$_6$) (1 b):** A solution of [Ir(dfppy)$_2$(bpy-DA)](PF$_6$) (51 mg, 48.8 μmol) in CH$_2$Cl$_2$ (20 mL) was purged with NO under ambient conditions for 10 min. The solution was evaporated to dryness. The residual solid was dissolved in CH$_2$Cl$_2$/MeOH (30 mL, 1:1, v/v) containing KPF$_6$ (9.89 mg, 53.7 μmol) and stirred for 30 min. The solvent was removed, and the resultant yellow solid was purified by column chromatography on silica gel using CH$_2$Cl$_2$/MeOH (30:1, v/v) as the eluent. Complex **1 b** was subsequently recrystallized from CH$_2$Cl$_2$/Et$_2$O to afford light yellow crystals (32 mg, 45%): $^1$H NMR (300 MHz, [D$_4$]methanol, 298 K, TMS): $\delta$ = 8.73 (s, 1H, H3 of bpy), 8.56 (s, 1H, H3′ of bpy), 8.37–8.32 (m, 2H, H6 of pyridyl ring of dfppy), 7.98–7.84 (m, 5H, H3 and H5 of pyridyl ring of dfppy, H6 of bpy), 7.71 (d, J = 6.0 Hz, 1H, H6′ of bpy), 7.66 (d, J = 6.0 Hz, 1H, H5 of bpy), 7.47 (d, J = 7.6 Hz, 1H, H4 of benzotriazole), 7.33 (d, J = 6.0 Hz, 1H, H5′ of bpy), 7.19–7.06 (m, 4H, H4 of pyridyl ring of dfppy, H5 and H7 of benzotriazole), 6.73–6.62 (m, 2H, H6 of phenyl ring of dfppy), 6.14 (s, 2H, CH$_2$), 5.69–5.66 (m, 2H, H4 of phenyl ring of dfppy), 3.86 (s, 3H, OCH$_3$), 2.59 ppm (s, 3H, CH$_3$ of bpy); IR (KBr): $\tilde{v}$ = 3448 (O—H), 848 cm$^{-1}$ (PF$_6^-$); MS (ESI$^+$): m/z (%): 904 (100) [M−PF$_6^-$]$^+$; Anal. calcd for IrC$_{41}$H$_{29}$N$_7$OPF$_{10}$·H$_2$O·(CH$_3$CH$_2$)$_2$O: C 47.37, H 3.62, N 8.59, found: C 47.03, H 3.62, N 8.99.

**[Ir(ppy)$_2$(bpy-T)](PF$_6$) (2 b):** The synthetic procedure was performed as described for complex **1 b**; however, [Ir(ppy)$_2$(bpy-DA)](PF$_6$) (70.0 mg, 72.4 μmol) was used instead of [Ir(dfppy)$_2$(bpy-DA)](PF$_6$). The crude product was purified by column chromatography on silica gel using CH$_2$Cl$_2$/MeOH (50:1, v/v) as the eluent and subsequently recrystallized from CH$_2$Cl$_2$/Et$_2$O afforded complex **2 b** as yellow crystals (20 mg, 28%): $^1$H NMR (400 MHz, [D$_4$]methanol, 298 K, TMS): $\delta$ = 8.68 (s, 1H, H3 of bpy), 8.51 (s, 1H, H3′ of bpy), 8.11 (t, J = 8.0 Hz, 2H, H3 of pyridyl ring of ppy), 7.97 (d, J = 5.6 Hz, H5 of bpy), 7.90–7.79 (m, 6H, H5′ and H6 of bpy, H4 of pyridyl ring, H3 of phenyl ring of ppy), 7.66–7.61 (m, 2H, H6 of pyridyl ring of ppy), 7.41 (d, J = 5.6 Hz, 1H, H6′ of bpy), 7.30 (d, J = 2.0 Hz, 1H, H4 of benzotriazole), 7.17 (d, J = 2.0 Hz, 1H, H7 of benzotriazole), 7.09 (dd, J = 9.2, 2.4 Hz, 1H, H5 of benzotriazole), 7.06–7.00 (m, 4H, H5 of pyridyl ring, H4 of phenyl ring of ppy), 6.88–6.86 (m, 2H, H5 of phenyl ring of ppy), 6.27 (d, J = 7.6 Hz, 2H, H6 of phenyl ring of ppy), 6.12 (s, 2H, CH$_2$), 3.86 (s, 3H, OCH$_3$), 2.58 ppm (s, 3H, CH$_3$ of bpy); IR (KBr): $\tilde{v}$ = 3448 (O—H), 844 cm$^{-1}$ (PF$_6^-$); MS (ESI$^+$): m/z (%): 832 (100) [M−PF$_6^-$]$^+$; Anal. calcd for IrC$_{41}$H$_{33}$N$_7$OPF$_6$·H$_2$O·2CH$_3$OH: C 48.77, H 4.09, N 9.26, found: C 49.18, H 4.29, N 9.45.

**[Ir(pq)$_2$(bpy-T)](PF$_6$) (3 b):** The synthetic procedure was performed as described for complex **1 b**; however, [Ir(pq)$_2$(bpy-DA)](PF$_6$) (69.8 mg, 65.5 μmol) was used instead of [Ir(dfppy)$_2$(bpy-DA)](PF$_6$). The crude product was purified by column chromatography on silica gel using n-hexane/EtOAc (1:1, v/v) as the eluent and subsequently recrystallized from CH$_2$Cl$_2$/Et$_2$O afforded complex **3 b** as orange crystals (21 mg, 30%): $^1$H NMR (300 MHz, [D$_4$]methanol, 298 K, TMS): $\delta$ = 8.36–8.24 (m, 5H, H3 of quinoline and H3 of phenyl ring of pq, H3 of bpy), 8.16–8.04 (m, 5H, H4 of quinoline, H3′, H6 and H6′ of bpy), 7.87 (d, J = 9.0 Hz, 1H, H4 of benzotriazole), 7.81–7.71 (m, 2H, H8 of quinoline of pq), 7.39–7.21 (m, 6H, H5 and H7 of quinoline of pq, H5 of bpy, H7 of benzotriazole), 7.16–7.07 (m, 3H, H4 of phenyl ring of pq, H5′ of bpy), 7.03–6.69 (m, 2H, H6

of quinoline of pq), 6.84–6.71 (m, 3H, H5 of benzotriazole, H5 of phenyl ring of pq), 6.46 (t, J = 7.2 Hz, 2H, H6 of phenyl ring of pq), 5.96 (s, 2H, CH$_2$), 3.78 (s, 3H, OCH$_3$), 2.42 ppm (s, 3H, CH$_3$ of bpy); IR (KBr): $\tilde{v}$ = 844 cm$^{-1}$ (PF$_6^-$); MS (ESI$^+$): m/z (%): 933 (100) [M−PF$_6^-$]$^+$; Anal. calcd for IrC$_{49}$H$_{37}$N$_7$OPF$_6$·2H$_2$O·CH$_3$OH: C 52.44, H 3.96, N 8.56, found: C 52.54, H 4.29, N 8.76.

**[Ir(pqe)$_2$(bpy-T)](PF$_6$) (4 b):** The synthetic procedure was performed as described for complex **1 b**; however, [Ir(pqe)$_2$(bpy-DA)](PF$_6$) (75.1 mg, 63.5 μmol) was used instead of [Ir(dfppy)$_2$(bpy-DA)](PF$_6$). The crude product was purified by column chromatography on silica gel using n-hexane/EtOAc (1:2, v/v) as the eluent and subsequently recrystallized from CH$_2$Cl$_2$/Et$_2$O afforded complex **4 b** as blood red crystals (20 mg, 26%): $^1$H NMR (400 MHz, [D$_6$]acetone, 298 K, TMS): $\delta$ = 8.84 (s, 1H, H3 of quinoline of pqe), 8.81 (s, 1H, H3 of quinoline of pqe), 8.52–8.50 (m, 3H, H5 of quinoline of pqe and H3 of bpy), 8.31–8.26 (m, 4H, H3 of phenyl ring of pqe and H3′ and H6 of bpy), 8.18 (d, J = 5.6 Hz, 1H, H6′ of bpy), 7.92 (d, J = 9.2 Hz, 1H, H5 of benzotriazole), 7.62–7.37 (m, 6H, H5 and H5′ of bpy, H6 and H8 of quinloine of pqe), 7.24–7.16 (m, 3H, H4 of phenyl ring and H7 of quinoline of pqe), 7.11–7.05 (m, 2H, H4 and H7 of benzotriazole), 6.95 (t, J = 7.2 Hz, 1H, H7 of quinoline of pqe), 6.89–6.82 (m, 2H, H5 of phenyl ring of pqe), 6.60 (d, J = 7.6 Hz, 2H, H6 of phenyl ring of pqe), 6.07 (s, 2H, CH$_2$), 4.13 (s, 6H, CO$_2$CH$_3$), 3.79 (s, 3H, OCH$_3$), 2.45 ppm (s, 3H, CH$_3$ of bpy); IR (KBr): $\tilde{v}$ = 3448 (O—H), 844 cm$^{-1}$ (PF$_6^-$); MS (ESI$^+$): m/z (%): 1048 (100) [M−PF$_6^-$]$^+$; Anal. calcd for IrC$_{53}$H$_{41}$N$_7$O$_5$PF$_6$·2H$_2$O·CH$_3$OH: C 51.43, H 3.92, N 7.77, found: C 53.36, H 4.18, N 7.70.

### Physical measurements and instrumentation

$^1$H NMR spectra were recorded on a Bruker 400 MHz NMR spectrometer at 298 K. Positive-ion electrospray ionization (ESI$^+$) mass spectra were recorded on a PerkinElmer Sciex API 365 mass spectrometer. IR spectra of the samples in KBr pellets were recorded in the range of 4000–400 cm$^{-1}$ using a PerkinElmer FTIR-1600 spectrophotometer. Elemental analyses were carried out on an Elementar Analysensysteme GmbH Vario MICRO elemental analyzer. The electrochemical measurements were performed on a CH Instruments Electrochemical Workstation CHI750A. Cyclic voltammetry experiments were carried out at RT using a two-compartment glass cell with a working volume of 500 μL. A platinum gauze counter electrode was accommodated in the working electrode compartment. The working and reference electrodes were a glassy carbon electrode and a Ag/AgNO$_3$ (0.1 M TBAP in CH$_3$CN) electrode, respectively. The reference electrode compartment was connected to the working electrode compartment via a Luggin capillary. Solutions for electrochemical measurements were degassed with prepurified nitrogen gas. All potentials were referred to SCE. Electronic absorption and steady-state emission spectra were recorded on a Hewlett–Packard 8453 diode array spectrophotometer and a SPEX FluoroLog 3-TCSPC spectrophotometer, respectively. Emission lifetimes were measured in the Fast MCS or TCSPC mode with a NanoLED N-375 as the excitation source. Unless specified, all solutions for photophysical studies were degassed with no fewer than four successive freeze-pump-thaw cycles and stored in a 10 cm$^3$ round-bottomed flask equipped with a side arm 1 cm fluorescence cuvette and sealed from the atmosphere by a Rotaflo HP6/6 quick-release Teflon stopper. Luminescence quantum yields were measured by the optically dilute method[32] with an aerated aqueous solution of [Ru(bpy)$_3$]Cl$_2$ ($\Phi_{em}$ = 0.028) as the standard solution.[33] Cell lysis was performed by probe sonication using a 130 watt ultrasonic processor with timer and pulser (Sonics & Materials, Inc., USA).

The self-quenching rate constants ($k_{sq}$) of the complexes in $CH_3CN$ were obtained by fitting the experimental data to the following equation:

$$\frac{1}{\tau} = \frac{1}{\tau_{i.d.}} + k_{sq}[Ir]$$

where $\tau$ is the emission lifetime of the complex at concentration [Ir] and $\tau_{i.d.}$ is the emission lifetime of the complex at infinite dilution.

Stern–Volmer quenching was studied by measuring the emission lifetimes of the complexes in $CH_3CN$ in the presence of the quencher (2-amino-4-methoxyaniline) at a concentration [Q]. The data were treated by a Stern–Volmer fit as follows:

$$\frac{\tau_o}{\tau} = 1 + k_q \tau_o [Q]$$

where $\tau_o$ and $\tau$ are the excited-state lifetimes of the complexes in the absence and presence of quencher, respectively, and $k_q$ is the bimolecular quenching rate constant. The corrected bimolecular quenching rate constants ($k_{sq'}$ and $k_{q'}$) were obtained from: $1/k_{sq'} = 1/k_{sq} - 1/k_d$ and $1/k_{q'} = 1/k_q - 1/k_d$, where $k_d$ is the diffusion-limited rate constant ($2.0 \times 10^{10}$ $dm^3 mol^{-1} s^{-1}$) for $CH_3CN$.

**pH-Dependent emission studies**: A 20 mL stock solution of complexes **2a** or complex **2b** (5 μM) in a mixture of 10 mM KOH and 100 mM KCl(aq)/MeOH (6:4, v/v) was prepared. The pH of the stock solution was adjusted to a desired value by addition of appropriate amounts of 10, 5, 2.5, 1.25, 0.5, 0.25, 0.13, 0.07, 0.04 or 0.02 N HCl(aq). After that, 2 mL of the stock solution was transferred to a quartz cuvette, and the emission spectrum was measured. The solution was then returned to the stock, and the pH was further adjusted. The overall increase in the volume of the stock solution due to pH adjustment was kept below 2%.

**NO-Sensing and selectivity studies**: All experiments were performed in potassium phosphate buffer (50 mM, pH 7.4)/DMSO (99:1, v/v) at RT. Various amounts of NOC-7 (2.5 mM; 0–20 μL) was added to a series of buffer solutions containing complex **2a** (5 μM). The reaction mixtures were gently stirred in the dark at RT for 1.5 h, and their emission spectra were recorded. In the selectivity studies, reactive oxygen and nitrogen species (RONS; 100 μM unless specified) were administrated to the buffer solutions of complex **2a** as follows. Nitrite ($NO_2^-$), nitrate ($NO_3^-$), superoxide ($O_2^-$), hypochlorite ($ClO^-$), and peroxynitrite ($ONOO^-$) were delivered from $NaNO_2$, $NaNO_3$, $KO_2$, $NaClO$, and $ONO_2Na$, respectively. The concentration of the $ONOO^-$ stock solution was determined by measuring its molar absorbance at 302 nm (extinction coefficient = 1670 $M^{-1} cm^{-1}$).[34] $H_2O_2$ was diluted immediately from a stabilized 30% aqueous solution. Hydroxyl radicals ($OH^\bullet$) were generated by the reaction of ammonium iron(II) sulfate hexahydrate and $H_2O_2$.[35] Singlet oxygen ($^1O_2$) was chemically generated from the $ClO^-/H_2O_2$ system.[36] All reaction mixtures were gently stirred in the dark at RT for 1.5 h before emission measurements.

**Lipophilicity**: The lipophilicity (log $P_{o/w}$) of the iridium(III) diamine complexes was determined using the flask-shaking method.[37] An aliquot of a stock solution of the complex in octan-1-ol (saturated with 0.9% NaCl, w/v) was added to an equal volume of aq NaCl (0.9%, w/v) (saturated with octan-1-ol). The mixture was swirled at 60 rpm for 30 min to allow partitioning at 298 K. The solution was then centrifuged, and the amounts of complex in organic layer ([Ir]$_o$) was determined by emission spectroscopy. The partition coefficient ($P_{o/w}$) for each complex was calculated as the ratio of [Ir]$_o$/

[Ir]$_w$, where [Ir]$_w$ was obtained by subtraction of the total amount of complex by the amount in the organic phase after partitioning.

### Biology

*Cell cultures*: HeLa cells and RAW 264.7 murine macrophages were cultured in high glucose DMEM (growth medium) supplemented with 10% FBS and 1% penicillin/streptomycin in a humidified chamber at 37 °C under a 5% $CO_2$ atmosphere. They were subcultured every 2–3 days.

*ICP-MS analyses*: HeLa cells grown in a 60-mm tissue culture dish were incubated with the iridium(III) diamine complexes (10 μM) in growth medium/DMSO (99:1, v/v) at 37 °C under a 5% $CO_2$ atmosphere for 4 h. The medium was removed, and the cell layer was washed gently with PBS (3×1 mL). The cells were trypsinized and harvested with PBS. The resultant solution (1 mL) was heated with 65% $HNO_3$ (1 mL) at 70 °C for 2 h, cooled to RT, and analyzed using an Elan 6100 DCR-ICP-MS (PerkinElmer SCIEX Instruments).

*Cell viability studies*: The cytotoxic effects of the iridium(III) diamine complexes were assessed using the MTT assay.[38] HeLa cells were seeded in a 96-well flat-bottomed microplate (≈10 000 cells/well) in growth medium (100 μL) and incubated at 37 °C under 5% $CO_2$ atmosphere for 24 h. Subsequently, the complexes (10 μM) were added to the wells in a mixture of growth medium/DMSO (99:1, v/v). Wells containing untreated cells were used as blank controls. The microplate was further incubated for 4 h. Then, 10 μL of MTT in PBS (5 mg mL$^{-1}$) was added to each well. The microplate was then incubated for another 4 h. The medium was removed carefully, and DMSO (200 μL) was added to each well. The microplate was further incubated for 10 min. The absorbance of the solutions at 570 nm was measured with a SPECTRAmax 340 microplate reader (Molecular Devices Corp., Sunnyvale, CA). Percentage cell survival was calculated relative to the absorbance of the control for each treatment. The viability of untreated cells was assumed to be 100%. The MTT assay for RAW 264.7 cells was performed by the same method, except complex **2a** (5 μM) and longer incubation time (3–24 h) were employed.

*Live-cell imaging of intracellular NO and co-staining experiment*: In the exogenous cellular NO imaging experiments, HeLa cells in growth medium were seeded on a sterilized coverslip in a 35-mm tissue culture dish and grown at 37 °C under 5% $CO_2$ atmosphere for 48 h. The culture medium was removed and replaced with growth medium/DMSO (99:1, v/v) containing complex **2a** (5 μM) for 1 h. The stained cells were washed with PBS (3×1 mL), and further treated with NOC-7 (100 μM) in PBS/FBS (99:1, v/v) for another 1 h. Prior to imaging, the cells were washed with PBS (3×1 mL) and mounted onto a sterilized glass slide. For endogenous cellular NO imaging experiments, RAW 264.7 murine macrophages were plated into a sterilized coverslip in a 35-mm tissue culture dish containing growth medium. After incubation at 37 °C under 5% $CO_2$ atmosphere for 48 h, the medium was removed, the cells were washed with PBS (3×1 mL), and incubated in 3 mL of fresh medium containing LPS (1 μg mL$^{-1}$) with or without L-NNA (1 mM) for 18 h. Cells were further incubated with complex **2a** for 1 h. Prior to imaging, cells were washed with PBS (1 mL×3) and mounted onto a sterilized glass slide. Unless specified, all imaging experiments were performed on a Leica TCS SPE confocal microscope with an oil immersion 40× or 63× objective and an excitation wavelength at 405 nm. The emission was measured using a long-pass filter at 532 nm. The excitation wavelength for imaging experiments involving MitoTracker Deep Red FM was 633 nm. The

Pearson's coefficient was determined by the program Image J (version 1.45k).

*ESI-MS analysis of cell extracts*: HeLa cells grown for 48 h were incubated with complex **2a** (5 μM) in growth medium/DMSO (99:1, *v/v*) at 37 °C for 1 h. The stained cells were washed with PBS (3× 1 mL), and further treated with NOC-7 (100 μM) in PBS/FBS (99:1, *v/v*) for 1 h. The solution was removed, and the cell layer was washed gently with PBS (3×1 mL). Cells were trypsinized and harvested with PBS (4×1 mL), and finally lysed by probe sonication with 90 cycles of 10 seconds on, 10 seconds off, at 80% power on an ice bath. The mixture was extracted with $CH_2Cl_2$ (3×4 mL). The combined organic layer was dried over $MgSO_4$, concentrated in vacuo, and analyzed by ESI-MS.

## Acknowledgements

**Keywords:** bioimaging · cellular probes · iridium · nitric oxide · phosphorescence

[1] a) W. P. Arnold, C. K. Mittal, S. Katsuki, F. Murad, *Proc. Natl. Acad. Sci. USA* **1977**, *74*, 3203–3207; b) L. J. Ignarro, G. M. Buga, K. S. Wood, R. E. Byrns, G. Chaudhuri, *Proc. Natl. Acad. Sci. USA* **1987**, *84*, 9265–9269; c) R. M. J. Palmer, A. G. Ferrige, S. Moncada, *Nature* **1987**, *327*, 524–526; d) R. F. Furchgott, *Angew. Chem.* **1999**, *111*, 1990–2000; *Angew. Chem. Int. Ed.* **1999**, *38*, 1870–1880; e) A. W. Carpenter, M. H. Schoenfisch, *Chem. Soc. Rev.* **2012**, *41*, 3742–3752.

[2] a) D. S. Bredt, P. M. Hwang, S. H. Snyder, *Nature* **1990**, *347*, 768–770; b) A. M. Leone, R. M. J. Palmer, R. G. Knowles, P. L. Francis, D. S. Ashton, S. Moncada, *J. Biol. Chem.* **1991**, *266*, 23790–23795; c) S. Pfeiffer, B. Mayer, B. Hemmens, *Angew. Chem.* **1999**, *111*, 1824–1844; *Angew. Chem. Int. Ed.* **1999**, *38*, 1714–1731; d) T. Nagano, *Chem. Rev.* **2002**, *102*, 1235–1269.

[3] a) S. Moncada, R. M. J. Palmer, E. A. Higgs, *Pharmacol. Rev.* **1991**, *43*, 109–142; b) J. F. Kerwin, J. R. Lancaster Jr., P. L. Feldman, *J. Med. Chem.* **1995**, *38*, 4343–4362; c) L. J. Ignarro, *Angew. Chem.* **1999**, *111*, 2002–2013; *Angew. Chem. Int. Ed.* **1999**, *38*, 1882–1892; d) L. J. Ignarro, *Nitric Oxide Biology and Pathobiology, 1st ed.*, Academic Press, San Diego, **2000**; e) J. E. Garthwaite, *Neuroscience* **2008**, *27*, 2783–2802; f) M. D. Pluth, E. Tomat, S. J. Lippard, *Annu. Rev. Biochem.* **2011**, *80*, 333–355.

[4] a) D. A. Wink, Y. Vodovotz, J. Laval, F. Laval, M. W. Dewhirst, J. B. Mitchell, *Carcinogenesis* **1998**, *19*, 711–721; b) M. A. Titheradge, *Biochim. Biophys. Acta Bioenerg.* **1999**, *1411*, 437–455; c) V. Calabrese, T. E. Bates, A. M. G. Stella, *Neurochem. Res.* **2000**, *25*, 1315–1341; d) G. C. Brown, A. Bal-Price, *Mol. Neurobiol.* **2003**, *27*, 325–355.

[5] a) L. C. Green, D. A. Wagner, J. Glogowski, P. L. Skipper, J. S. Wishnok, S. R. Tannenbaum, *Anal. Biochem.* **1982**, *126*, 131–138; b) R. W. Nims, J. F. Darbyshire, J. E. Saavedra, D. Christodoulou, I. Hanbauer, G. W. Cox, M. B. Grisham, F. Laval, J. A. Cook, M. C. Krishna, D. A. Wink, *Methods* **1995**, *7*, 48–54; c) L. A. Ridnour, J. E. Sim, M. A. Hayward, D. A. Wink, S. M. Martin, G. R. Buettner, D. R. Spitz, *Anal. Biochem.* **2000**, *281*, 223–229; d) F. Brown, N. J. Finnerty, F. B. Bolger, J. Millar, J. P. Lowry, *Anal. Bioanal. Chem.* **2005**, *381*, 964–971; e) H. Zheng, G. Q. Shang, S. Y. Yang, X. Gao, J. G. Xu, *Org. Lett.* **2008**, *10*, 2357–2360.

[6] a) T. Malinski, Z. Taha, *Nature* **1992**, *358*, 676–678; b) K. Ichimori, I. H. Shida, M. Fukahori, H. Nakazawa, E. Murakami, *Rev. Sci. Instrum.* **1994**, *65*, 2714–2717; c) F. Bedioui, N. Villeneuve, *Electroanalysis* **2003**, *15*, 5–18.

[7] a) M. H. Lim, S. J. Lippard, *Acc. Chem. Res.* **2007**, *40*, 41–51; b) E. W. Miller, C. J. Chang, *Curr. Opin. Chem. Biol.* **2007**, *11*, 620–625; c) M. D. Pluth, L. E. McQuade, S. J. Lippard, *Org. Lett.* **2010**, *12*, 2318–2321; d) Y. Yang, S. K. Seidlits, M. M. Adams, V. M. Lynch, C. E. Schmidt, E. V. Anslyn, J. B. Shear, *J. Am. Chem. Soc.* **2010**, *132*, 13114–13116; e) T. Nagano, *Proc. Jpn. Acad. Ser. B* **2010**, *86*, 837–847; f) P. Kumar, A. Kalita, B. Mondal, *Dalton Trans.* **2011**, *40*, 8656–8663; g) C. Sun, W. Shi, Y. Song, W. Chen, H. Ma, *Chem. Commun.* **2011**, *47*, 8638–8640; h) X. Hu, J. Wang, X. Zhu, D. Dong, X. Zhang, S. Wu, C. Duan, *Chem. Commun.* **2011**, *47*, 11507–11509; i) M. D. Pluth, M. R. Chan, L. E. McQuade, S. J. Lippard, *Inorg. Chem.* **2011**, *50*, 9385–9392; j) T.-W. Shiue, Y.-H. Chen, C.-M. Wu, G. Singh, H.-Y. Chen, C.-H. Hung, W.-F. Liaw, Y.-M. Wang, *Inorg. Chem.* **2012**, *51*, 5400–5408; k) E. W. Seo, J. H. Han, C. H. Heo, J. H. Shin, H. M. Kim, B. R. Cho, *Chem. Eur. J.* **2012**, *18*, 12388–12394; l) H. Yu, Y. Xiao, L. Jin, *J. Am. Chem. Soc.* **2012**, *134*, 17486–17489.

[8] a) K. Sancier, G. Freeman, I. Mills, *Science* **1962**, *137*, 752–754; b) H. Kosaka, H. Watanabe, H. Yoshihara, N. Harada, T. Shiga, *Biochem. Biophys. Res. Commun.* **1992**, *184*, 1119–1124; c) Y. Katayama, N. Soh, M. Maeda, *ChemPhysChem* **2001**, *2*, 655–661.

[9] J. F. Brien, B. E. McLaughlin, K. Nakatsu, G. S. Marks, *Methods Enzymol.* **1996**, *268*, 83–92.

[10] a) H. Kojima, N. Nakatsubo, K. Kikuchi, S. Kawahara, Y. Kirino, T. Nagano, *Anal. Chem.* **1998**, *70*, 2446–2453; b) H. Kojima, Y. Urano, K. Kikuchi, T. Higuchi, T. Nagano, *Angew. Chem.* **1999**, *111*, 3419–3422; *Angew. Chem. Int. Ed.* **1999**, *38*, 3209–3212.

[11] H. Kojima, M. Hirotani, N. Nakatsubo, K. Kikuchi, Y. Urano, T. Higuchi, H. Yasunobu, T. Nagano, *Anal. Chem.* **2001**, *73*, 1967–1973.

[12] a) Y. Gabe, Y. Urano, K. Kikuchi, H. Kojima, T. Nagano, *J. Am. Chem. Soc.* **2004**, *126*, 3357–3367; b) Y. Gabe, T. Ueno, Y. Urano, H. Kojima, T. Nagano, *Anal. Bioanal. Chem.* **2006**, *386*, 621–626.

[13] S. Izumi, Y. Urano, K. Hanaoka, T. Terai, T. Nagano, *J. Am. Chem. Soc.* **2009**, *131*, 10189–10200.

[14] E. Sasaki, H. Kojima, H. Nishimatsu, K. Kikuchi, Y. Hirata, T. Nagano, *J. Am. Chem. Soc.* **2005**, *127*, 3684–3685.

[15] a) R. Zhang, Z. Ye, G. Wang, W. Zhang, J. Yuan, *Chem. Eur. J.* **2010**, *16*, 6884–6891; b) Y. Chen, W. Guo, Z. Ye, G. Wang, W. Yuan, *Chem. Commun.* **2011**, *47*, 6266–6268; c) A. W.-T. Choi, C.-S. Poon, H.-W. Liu, H.-K. Cheng, K. K.-W. Lo, *New J. Chem.* **2013**, *37*, 1711–1719; d) A. W.-T. Choi, H.-W. Liu, K. K.-W. Lo, *unpublished results*.

[16] a) K. K.-W. Lo, J. S.-W. Chan, L.-H. Lui, C.-K. Chung, *Organometallics* **2004**, *23*, 3108–3116; b) M. Cavazzini, S. Quici, C. Scalera, F. Puntoriero, G. La Ganga, S. Campagna, *Inorg. Chem.* **2009**, *48*, 8578–8592; c) Q. Zhao, M. Yu, L. Shi, S. Liu, C. Li, M. Shi, Z. Zhou, C. Huang, F. Li, *Organometallics* **2010**, *29*, 1085–1091; d) R. A. Smith, E. C. Stokes, E. E. Langdon-Jones, J. A. Platts, B. M. Kariuki, A. J. Hallet, S. J. A. Pope, *Dalton Trans.* **2013**, *42*, 10347–10357.

[17] a) S. Welter, S. Lafolet, E. Cecchetto, F. Vergeer, L. De Cola, *ChemPhysChem* **2005**, *6*, 2417–2427; b) F. De Angelis, S. Fantacci, N. Evans, C. Klevin, S. M. Zakeeruddin, J.-E. Moser, K. Kalyanasundarma, H. J. Bolink, M. Grätzel, M. K. Nazeeruddin, *Inorg. Chem.* **2007**, *46*, 5989–6001.

[18] a) S. Sprouse, K. A. King, P. J. Spellane, R. J. Watts, *J. Am. Chem. Soc.* **1984**, *106*, 6647–6653; b) A. P. Wilde, R. J. Watts, *J. Phys. Chem.* **1991**, *95*, 622–629; c) M. Maestri, V. Balzani, C. Deuschel-Cornioley, A. von Zelewsky, *Adv. Photochem.* **1992**, *17*, 1–68; d) L. Flamigni, A. Barbieri, C. Sabatini, B. Ventura, F. Barigelletti, *Top. Curr. Chem.* **2007**, *281*, 143–203.

[19] K. K.-W. Lo, A. W.-T. Choi, W. H.-T. Law, *Dalton Trans.* **2012**, *41*, 6021–6047.

[20] a) K. K.-W. Lo, K. Y. Zhang, S.-K. Leung, M.-C. Tang, *Angew. Chem.* **2008**, *120*, 2245–2248; *Angew. Chem. Int. Ed.* **2008**, *47*, 2213–2216; b) S.-K. Leung, K. Y. Kwok, K. Y. Zhang, K. K.-W. Lo, *Inorg. Chem.* **2010**, *49*, 4984–4995; c) S.-K. Leung, H.-W. Liu, K. K.-W. Lo, *Chem. Commun.* **2011**, *47*, 10548–10550; d) S. Ladouceur, L. Donato, M. Romain, B. P. Mudraboyina, M. B. Johansen, J. A. Wisner, E. Zysman-Colman, *Dalton Trans.* **2013**, *42*, 8838–8847.

[21] a) K. K.-W. Lo, K. Y. Zhang, C.-K. Chung, K. Y. Kwok, *Chem. Eur. J.* **2007**, *13*, 7110–7120; b) H.-W. Liu, K. Y. Zhang, W. H.-T. Law, *Organometallics*

**2010**, *29*, 3474–3476; c) K. K.-W. Lo, S. P.-Y. Li, K. Y. Zhang, *New J. Chem.* **2011**, *35*, 265–287.

[22] a) T. Miura, Y. Urano, K. Tanaka, T. Nagano, K. Ohkubo, S. Fukuzumi, *J. Am. Chem. Soc.* **2003**, *125*, 8666–8671; b) D. P. Kennedy, C. M. Kormos, S. C. Burdette, *J. Am. Chem. Soc.* **2009**, *131*, 8578–8586.

[23] P. M. Dewick, *Essentials of Organic Chemistry: For Students of Pharmacy, Medicinal Chemistry and Biological Chemistry*, Wiley, Chichester, **2006**.

[24] D. A. Wink, L. K. Keefer, *J. Org. Chem.* **1993**, *58*, 1472–1476.

[25] a) J. J. Haddad, *Biochem. Biophys. Res. Commun.* **2004**, *316*, 969–977; b) T. Nagano, *J. Clin. Biochem. Nutr.* **2009**, *45*, 111–124; c) P. Newsholme, E. Rebelato, F. Abdulkader, M. Krause, A. Carpinelli, R. Curi, *J. Endocrinol.* **2012**, *214*, 11–20.

[26] a) K. Y. Zhang, K. K.-W. Lo, *Inorg. Chem.* **2009**, *48*, 6011–6025; b) K. Y. Zhang, H.-W. Liu, T. T.-H. Fong, X.-G. Chen, K. K.-W. Lo, *Inorg. Chem.* **2010**, *49*, 5432–5443.

[27] a) T. Kobayashi, Y. Arakawa, *J. Cell Biol.* **1991**, *113*, 235–244; b) R. E. Pagano, O. C. Martin, H.-C. Kang, R. P. Haugland, *J. Cell Biol.* **1991**, *113*, 1267–1279.

[28] C. Bogdan, *Nat. Immunol.* **2001**, *2*, 907–916.

[29] E. S. Furfine, M. F. Harmon, J. E. Paith, E. P. Garvey, *Biochemistry* **1993**, *32*, 8512–8517.

[30] W. L. F. Armarego, C. L. L. Chai, *Purification of Laboratory Chemicals*, 6th ed., Elsevier, Oxford, **2009**.

[31] a) M. Nonoyama, *Bull. Chem. Soc. Jpn.* **1974**, *47*, 767–768; b) B. M. Peek, G. T. Ross, S. W. Edwards, G. J. Meyer, T. J. Meyer, B. W. Erickson, *Int. J. Peptide Res.* **1991**, *38*, 114–123; c) K. K.-W. Lo, C.-K. Chung, T. K.-M. Lee, L.-H. Lui, K. H.-K. Tsang, N. Zhu, *Inorg. Chem.* **2003**, *42*, 6886–6897.

[32] J. N. Demas, G. A. Crosby, *J. Phys. Chem.* **1971**, *75*, 991–1024.

[33] K. Nakamaru, *Bull. Chem. Soc. Jpn.* **1982**, *55*, 2697–2705.

[34] S. Miyamoto, G. R. Martinez, A. P. B. Martins, M. H. G. Medeiros, P. D. Mascio, *J. Am. Chem. Soc.* **2003**, *125*, 4510–4517.

[35] K. Setsukinai, Y. Urano, K. Kakinuma, H. J. Majima, T. Nagano, *J. Biol. Chem.* **2003**, *278*, 3170–3175.

[36] a) A. M. Held, D. J. Halko, J. K. Hurst, *J. Am. Chem. Soc.* **1978**, *100*, 5732–5740; b) J. M. Aubry, *J. Am. Chem. Soc.* **1985**, *107*, 5844–5849.

[37] M. J. McKeage, S. J. Berners-Price, P. Galettis, R. J. Bowen, W. Brouwer, L. Ding, L. Zhuang, B. C. Baguley, *Cancer Chemother. Pharmacol.* **2000**, *46*, 343–350.

[38] T. Mosmann, *J. Immunol. Methods* **1983**, *65*, 55–63.